JPET Fast Forward. Published on March 25, 2019 as DOI: 10.1124/jpet.118.250126
This article has not been copyedited and formatted. The final version may differ from this version.

Modulation of TARP γ8-containing AMPA Receptors as a Novel Therapeutic Approach for Chronic Pain*

Kelly L Knopp, Rosa Maria A Simmons, Wenhong Guo, Benjamin L Adams, Kevin M Gardinier, Douglas L Gernert, Paul L Ornstein, Warren Porter, Jon Reel, Chunjin Ding, He Wang, Yuewei Qian, Kevin D Burris, Anne Need, Vanessa Barth, Steven Swanson, John Catlow, Jeffrey M Witkin, Ruud Zwart, Emanuele Sher, Kar-Chan Choong, Theron M Wall, Douglas Schober, Christian C Felder, Akihiko S Kato, David S Bredt, Eric S Nisenbaum

Primary laboratory of origin: Lilly Research Laboratories, Eli Lilly and Company, Indianapolis, IN 46285, USA.

Lilly Research Laboratories, Eli Lilly and Company, Indianapolis, IN 46285, USA: KLK, RMAS, WG, BLA, KMG, DLG, PLO, WP, JR, CD, HW, YQ, KDB, AN, VB, SS, JC, JMW, K-CC, TMW, DS, CCF, ASK, DSB, ESN

Lilly Research Centre, Eli Lilly and Company Ltd., Erl Wood Manor, Windlesham, Surrey GU20 6PH, UK: RZ, ES

Present addresses:

ESN: CNS Discovery Reseasrch, Alkermes Inc. 852 Winter Street, Waltham, MA 02451

KMG: Global Discovery Chemistry, Novartis Institutes for BioMedical Research, 22 Windsor Street, Cambridge, MA 02139

PLO: Medicinal Chemistry School of Pharmacy Medical College of Wisconsin, 8701 Watertown Plank Road, Milwaukee, WI 53226

DSB: Neuroscience Discovery, Janssen Pharmaceutical Companies of Johnson & Johnson, 3210 Merryfield Row, San Diego, CA 92121, USA.

JPET Fast Forward. Published on March 25, 2019 as DOI: 10.1124/jpet.118.250126
This article has not been copyedited and formatted. The final version may differ from this version.

Running Title:

Blockade of TARP γ8-AMPA receptors is antinociceptive

Corresponding Author: Kelly L. Knopp, Lilly Research Laboratories, Indianapolis, IN 46285, 317-277-0210 (t), 317-276-7600, k.knopp@lilly.com

Number of Text Pages:
Number of Tables: 0
Number of Figures: 13
Number of References: 63
Number of Words in Abstract: 250
Number of Words in Introduction: 518
Number of Words in Discussion: 1495

Abbreviations:
ACC: anterior cingulate cortex
AMPA: α-amino-3-hydroxy-5-methyl-4-isoxazolepropionic acid
CFA: Complete Freund's Adjuvant
SS: somatosensory
TARP: transmembrane AMPA receptor regulatory proteins

Recommended Assignment:
Drug Discovery and Translational Medicine

JPET Fast Forward. Published on March 25, 2019 as DOI: 10.1124/jpet.118.250126
This article has not been copyedited and formatted. The final version may differ from this version.

Abstract

Non-selective glutamate AMPA receptor antagonists are efficacious in chronic pain, but have significant tolerability issues, likely arising from the ubiquitous expression of AMPA receptors in CNS. Recently, LY3130481 has been shown to selectively block AMPA receptors co-assembled with the auxiliary protein, TARP γ8, which is highly expressed in hippocampus, but also in pain pathways, including anterior cingulate (ACC) and somatosensory (SS) cortices and spinal cord, suggesting that selective blockade γ8/AMPA receptors may suppress nociceptive signaling with fewer CNS side effects. The potency of LY3130481 on recombinant γ8-containing AMPA receptors was modulated by co-expression with other TARPs; γ2 subunits affected activity more than γ3 subunits. Consistent with these findings, LY3130481 had decreasing potency on receptors from rat hippocampal, cortical, spinal cord, and cerebellar neurons that was replicated in tissue from human brain. LY3130481 partially suppressed, whereas the non-selective AMPA antagonist GYKI53784 completely blocked AMPA receptor-dependent EPSPs in ACC and spinal neurons in vitro. Similarly, LY3130481 attenuated short-term synaptic plasticity in spinal sensory neurons in vivo in response stimulation of peripheral afferents. LY3130481 also significantly reduced nocifensive behaviors after intraplantar formalin that was correlated with occupancy of CNS γ8-containing AMPA receptors. In addition, LY3130481 dose-dependently attenuated established gait impairment after joint damage and tactile allodynia after spinal nerve ligation; all in the absence of motor side effects. Collectively, these data demonstrate that LY3130481 can suppress excitatory synaptic transmission and plasticity in pain pathways containing γ8/AMPA receptors and significantly reduce nocifensive behaviors, suggesting a novel, effective and safer therapy for chronic pain conditions.

JPET Fast Forward. Published on March 25, 2019 as DOI: 10.1124/jpet.118.250126
This article has not been copyedited and formatted. The final version may differ from this version.

1. Introduction

Although the etiology of chronic pain is diverse (e.g., tissue injury, inflammation), a long-term sensitization of the central somatosensory pathways is common to many disorders and is characterized by increased neuronal excitability and enhanced synaptic transmission in nociceptive and non-nociceptive pathways that underlies the hallmark symptoms of allodynia, hyperalgesia and spontaneous pain (Latremoliere A, 2009). While multiple mechanisms contribute to central sensitization, the release of glutamate from peripheral nerve terminals, activation of ionotropic glutamate AMPA receptors and subsequent recruitment of NMDA receptor activity in the dorsal horn of the spinal cord is critical for the initiation and maintenance of enhanced synaptic transmission in central pain pathways (Davies SN, 1987; Yoshimura M, 1990; Woolf CJ, 1991). Consistent with the role of AMPA receptors in central sensitization, clinical studies have demonstrated that compounds with AMPA receptor antagonist properties (e.g., tezampanel, topiramate, NS1209) can attenuate the symptoms of chronic pain, but are accompanied by significant tolerability issues (e.g., dizziness, sedation) (Wandschneider, 2017), probably due to the ubiquitous expression of AMPA receptors in CNS (Olsen RW, 1987). This hypothesis is supported by preclinical studies which have demonstrated that non-selective AMPA receptor antagonists reduce nocifensive behaviors at doses that also produce motor side effects and sedation (Simmons RM, 1998; Nishiyama T, 1999) .

AMPA receptors mediate the majority of fast excitatory transmission in the CNS and are tetramers composed of one or more , GluA1–4 subunits, that can have two alternative splice variants (flip and flop) (Sommer et al., 1990; Monyer et al., 1991) . Additional diversity is conferred by association with auxiliary subunits termed transmembrane AMPA receptor regulatory proteins (TARPs; γ2, γ3, γ4, γ5, γ7, and γ8) and cornichon proteins (CNIH-2, CNIH-3) that are heterogeneously expressed in the CNS and can influence channel kinetics, receptor trafficking and pharmacology (Schwenk et al., 2009; Jackson and Nicoll, 2011; Schwenk et al., 2012). Of the TARPs, γ8 has highest expression in hippocampus, but appreciable expression is also observed in regions associated with nociceptive processing, including

ACC and SS cortices, sensory thalamus and the dorsal horn of the spinal cord (Tomita et al., 2003; Fukaya et al., 2006; Inamura et al., 2006; Menuz et al., 2009; Larsson M, 2013). In these nociceptive regions, γ2 and γ3 TARPs are also expressed at relatively high levels (Tomita et al., 2003). Ultrastructural analyses have demonstrated that γ2 and γ8 subunits are localized to postsynaptic densities of presumptive excitatory synapses in cortex (Inamura et al., 2006), whereas γ2, γ3, γ4, γ7 and γ8 TARPs are expressed in spinal cord and γ8 is highly expressed at postsynaptic sites to primary afferents onto dorsal horn neurons (Larsson M, 2013; Sullivan SJ, 2017). Collectively, these data suggest that γ8-containing AMPA receptors may be important for establishing the activity-dependent sensitization of glutamatergic nociceptive inputs in spinal and supraspinal regions of the CNS.

Recently, a novel AMPA receptor antagonist, LY3130481, has been identified which selectively blocks TARP γ8-containing AMPA receptors (Gardinier et al., 2016; Kato and Witkin, 2018) . LY3130481 displays nanomolar potency for blockade of recombinant and native γ8-containing AMPA receptors and ≥100-fold selectivity versus AMPA receptors associated with other γ subunits or GluA subunits alone (Gardinier et al., 2016; Kato et al., 2016) . The compound also has pharmacokinetic properties suitable for testing *in vivo*, including high oral bioavailability, modest intrinsic clearance and high CNS exposure (Gardinier et al., 2016; Kato et al., 2016) . The present studies use LY3130481 to interrogate the hypothesis that selective blockade of γ8-containing AMPA receptors can reduce glutamatergic synaptic transmission in CNS somatosensory pathways and attenuate nocifensive responses in animal models of hyperexcitable neurotransmission with reduced CNS side-effects.

2. Methods

2.1 Experimental Animals

All animal studies were reviewed and approved by the Lilly Institutional Animal Care and Use Committee and conform to the Guidelines provided by the National Institutes of Health and the International Association for the Study of Pain. Animals were randomly assigned to treatment groups

and experimenters performing behavioral scoring were blinded to treatment (drug or genotype) assignment. The same experimenter performed all studies for a given assay.

Depending on body weight, rats were either grouped-housed or pair-housed in large high-density plexiglass cages with bedding and enrichment. Mice were group-housed in high-density large mouse plexiglass cages with bedding and enrichment. Animals were maintained in temperature- and humidity-controlled rooms on a 12-/12-hr light/dark cycle (lights on at 6:00 a.m.) and ad libitum access to food and water unless otherwise specified. All behavioral testing was conducted between 7:30 a.m. and 4:00 p.m. during the light cycle. The testing room temperature was maintained at 21-23º C.

2.2 Formalin Assay

Male Sprague Dawley (SD) rats (186-240 g) were utilized for the rat formalin assay (Charles River, Portage, MI, USA). CD-1 Icr mice (Harlan, Indianapolis, IN, USA) (32-43 g) were utilized for the mouse formalin studies. For the transgenic studies, mice were generated at Taconic (Cambridge City, IN, USA) on a CD1 background, weighing 24-37 g at the time of testing. The $\gamma 8^{+/+}$ and $\gamma 8^{-/-}$ mice were age-matched. The formalin assay was performed in custom-made Plexiglas boxes, 22 x 22 x 20 cm for rats, 12.5 x 12.5 x 12.5 cm for mice. A mirror placed at the back of the cage allowed the unhindered observation of the formalin-injected paw. Rats were habituated to the chambers for at least 30 min prior to the experiment, mice were habituated for 60 minutes. LY3130481 was administered p.o. 30 min before the formalin challenge, tramadol (p.o., 1 hr) and carbamazepine (i.p., 30 min). A 5% formalin solution in 0.9% saline (injection volume of 50 µl for rats, 20 µl for mice) was injected subcutaneously into the dorsal lateral surface of one hind paw with a 27 gauge needle for rats and into the plantar surface of one hind paw for mice. Real-time observation began immediately after the formalin injection. Formalin-induced nocifensive responding was quantified by recording the number of seconds of each licking/biting event, binned in 5-minute intervals for 60 min after the formalin injection. Two phases of pain behavior were observed as previously described (Wheeler-Aceto H, 1990). The early phase started immediately after the formalin injection and lasted approximately 5 min, followed by the late phase that

started between minutes 10-15 with a maximal response typically observed around 25-35 min after the formalin injection. After the 60 min observation period, animals were sacrificed with CO_2 followed by cervical dislocation as a secondary measure.

The total time spent licking and biting the injected paw (Coderre TJ, 1993; Abbott FV, 1995) (was recorded; the early phase score was the sum of time spent licking in seconds from 0 to 5 min, the late phase score was obtained by adding the total number of seconds spent licking from minute 16 to minute 40 of the observation period for rats, minute 16 to minute 55 for mice. Data are presented as means with standard errors of means (± SEM), and were evaluated by one-way analysis of variance (ANOVA) and the appropriate contrasts analyzed by Dunnett's t-test for two sided comparisons. Differences were considered to be significant if the p-value was less than 0.05.

2.3 *Gait Assay*

Female SD rats (Harlan, Indianapolis, IN, USA) (200-240 g) were utilized for the gait study. Rats were anesthetized with 4% isoflurane in oxygen and the rear right knee was shaved and sterilized with 70% ethanol. Injections were performed with a 27-gauge needle fitted with PE10 tubing such that 4 mm of the needle tip was exposed, thereby controlling injection depth. CFA (1 mg/ml concentration, Sigma-Aldrich, St. Louis, MO, Cat#: F-5881, lot#: 101k8927) was diluted with Freund's Incomplete Adjuvant (IFA, MP Biomedicals LLC, catalog #: 642861, lot#: 07263) to form a 0.4 mg/ml suspension. Each rat received 20 µg CFA in a 50 µL injection.

The GaitScan (CleverSys Inc., Reston, VA) gait analysis system recorded and quantified gait features, and the experimental procedure was conducted as previously described (Adams BL, 2016). Briefly, the system consisted of a clear treadmill (ExerGait XL, Columbus Instruments, OH, USA) fitted with an angled mirror underneath. A high-speed camera (Basler, 100 fps) recorded the ventral view of a moving rat. An opaque green plexiglass box with a semi-transparent viewing window was positioned above the treadmill to house the animal. Video was captured by the BCam software program for 2000 frames per

animal for analysis. This color-based tracking system allowed maximal tracking of the paw, while excluding other body parts or shadows. Filters were applied to enable the analysis of multiple steps per animal. An a priori inclusion criterion of a minimum of 3 strides per rear limb was required for all studies.

Prior to CFA administration, rats were habituated to the treadmill for 60 s. The treadmill was slowly increased from 0 to 2 cm/s. After the animal moved forward and away from back wall twice, the speed was slowly increased to 4 cm/s. Infrequently, a cotton swab was inserted into the front of the treadmill to re-orient a rat that was excessively rearing or exploring the chamber, effectively returning the rat to a normal walking pattern. As well, a rounded 'bumper' was placed on the back wall to minimize any negative impact of contact while the rat was learning the forced ambulation paradigm. Once the animal walked consistently, trial speeds were increased in increments of 2-3 cm/s until the animal successfully ran at or near 16 cm/s. The animal was then placed back in the home cage.

Rats received a baseline gait session the day after CFA administration (Day 2). The next day, rats were randomly assigned to groups and received one of the following treatments 60 min prior to the test session: Vehicle, 1, 3, 10, or 30 mg/kg LY3130481, or 40 mg/kg Tramadol HCl (4 ml/kg). All compounds were orally administered at 10 mL/kg. For the baseline and test sessions, the treadmill speeds were slowly ramped from 0 to the target speed of 12-16 cm/s, depending on the ability of the individual rat. Filters in the analysis software were implemented to exclude instances of pausing, rearing, turning, riding back, or when the rat was touching the rear of the treadmill, thereby decreasing the variability in gait measures and allowing a more accurate representation of locomotion.

2.4 Spinal Nerve Ligation (SNL) Assay

Male Sprague Dawley rats (Harlan, Indianapolis, IN) weighing 150-200 g at the time of surgery were acclimated for at least 4 days prior to surgery. Surgery was performed on Day 0 as described previously (Kim and Chung, 1992). Briefly, rats were placed under gas anesthesia using a mixture of

isoflurane (3% for induction, 2% for maintenance) and oxygen. Rats were placed in a prone position and the left paraspinal muscles were separated from the spinous processes at the L4-S2 levels. The L6 transverse process was carefully removed with a small rongeur to identify visually the L4-L6 spinal nerves. The left L5 and L6 spinal nerves were isolated and tightly ligated with 6-0 silk thread and the L4 spinal nerve is lightly tapped (up to 20 times) with a glass rod to produce adequate nerve injury. The muscle was then closed with 3-0 silk sutures, and wound clips were used to close superficial skin. After surgery, rats were returned to their home cages. As the surgery was conducted at Covance Laboratories (Greenfield, IN), the rats were shipped to Lilly Research Laboratories the day after surgery (day 1). A total of 33 rats underwent SNL surgery. On postoperative days 1, 3, 5, and 7, and weekly thereafter, the rat's left hind paw was lightly tapped/brushed with an innocuous mechanical stimuli to prime the onset of hypersensitivity as previously described (Simmons et al., 2014). After priming, baseline hypersensitivity was evaluated using the up-down method of paw withdrawal in response to von Frey filaments with incremental bending forces (0.3-15g) as previously described (Chaplan et al., 1994). Any rat that did not reach the predetermined inclusion criterion of a baseline response of <2g in the paw ipsilateral to the ligation was not included in the drug study. Treatment assignment was block randomized based on body weight. During the drug study beginning 31 days after nerve ligation surgery, rats were place in elevated observation chambers with wire mesh floor and allowed an acclimation period of 10-20 minutes before testing. Rats were administered vehicle, LY3130481, or the positive control gabapentin per os (p.o.), and tactile hypersensitivity was evaluated 0.5, 1 and 1.5 hours after administration. Dosing was continued for 4 more days, and hypersensitivity was again evaluated at 0.5 and 1 hour post-administration. All behavioral studies were conducted by a blinded observer. Data are expressed as the threshold force required to elicit a response (grams) and are expressed as means $\pm$ S.E.M. Statistical analysis was performed using JMP 8.0 software (SAS Institute Inc., Cary, NC) and were evaluated by one-way analysis of variance (ANOVA) and the appropriate contrasts analyzed by the Dunnett *t*-test for two-sided comparisons. Values of $p < 0.05$ were considered statistically significant.

2.5 *Drug Treatments for In Vivo Studies*

LY3130481 was prepared at 3 mg/ml for rats and at 0.5 or 1 mg/ml for mice by dissolving the compound in DMSO (5% of total volume), adding 10% Acacia and 0.05% Antifoam (Fisher Scientific, Custom Vehicles, Lot: 072012), and vortexing until solubilized for the formalin, rotorod and gait assays. The compound was serially diluted if needed and dosed at 10 ml/kg. For *in vivo* electrophysiological studies, LY3130481 was dissolved in 20% Captisol in water and sonicated for 45 min in a warm water bath.

GYKI52466 was synthesized at Eli Lilly. For the formalin and rotorod studies, GYKI52466 was prepared at 3 mg/ml in milliQ water and bath sonicated until solubilized. The compound was serially diluted if needed and dosed at 10 ml/kg i.p. For *in vivo* electrophysiological studies, GYKI52466 was dissolved in 0.9% saline and sonicated for 30 min in warm bath prior to i.v. administration via the jugular vein.

Tramadol HCl (Teva Pharmaceuticals) was prepared by sonicating crushed tablets in a 1% hydroxyethylcellulose, 0.25% Tween 80 and 0.05% Dow antifoam (HEC) for the gait study and in MilliQ water for the rat formalin study to form a suspension with the assumption that each tablet contained 50 mg of active drug. Rats were dosed 40 mg/kg (p.o.) in a dose volume of 4 mL/kg. Pre-treatment times were 1 hr prior to testing in the formalin and gait assays.

Gabapentin (Neurontin®, 400 mg capsules) was purchased from Capital Wholesale Drug Co (Columbus, OH). A 12.5 mg/ml suspension of Gabapentin was prepared by dissolving the contents of a 400 mg Neurontin® capsule in 32 mls of vehicle (Milli-Q (Millipore) water), and dosed at 75 mg/kg.

All drugs used for *in vivo* studies were prepared fresh daily.

2.6 *Pharmacokinetics*

Male, SD rats (Harlan, Indianapolis, IN, USA) weighing 250-270 gm and fasted for at least 12 hr were dosed p.o. with LY3130481 (3 mg/kg in a 10 mL/kg dose volume) or i.v. 1 mg/kg in a 1 mL/kg dose volume. The vehicle solutions for oral and intravenous delivery were Acacia, antifoam and propylene glycol or polyethylene glycol 400 80% v/v and N-methylpyrrolidone 20% v/v, respectively. Plasma samples (75-250 uL) were collected via cannulation of the femoral artery at time points of 0, 0.08, 0.25, 0.5, 1, 2, 3, 8, 12, and 24 hr post-dosing. Samples were placed into vials containing EDTA on ice, centrifuged and stored at $\leq$ -20^{o} C for later HPLC analysis.

2.7 *Receptor Occupancy*

Male SD rats (Harlan, Indianapolis, IN, USA) (200-240 g) were utilized for the receptor occupancy studies. Food and water were provided ad libitum but food was removed approximately 12 hr prior to p.o. administration. Rats (*n*=3-4) were administered either vehicle alone (10% acacia with 0.05% antifoam in purified water) or LY3130481 (0.1-30 mg/kg) via oral gavage in a dose volume of 10 mL/kg. Thirty minutes after receiving vehicle or compound they received i.v. administration of nonlabeled tracer (LY3075449, 3 μg/kg in 25% hydroxypropyl-beta-cyclodextran, 0.5 ml/kg dose volume) in the lateral tail vein. Rats were sacrificed by cervical dislocation forty min after nonlabled tracer administration. Brains were removed and the hippocampus and cerebellum were dissected, weighed and placed in conical centrifuge tubes on ice. The remaining brain and plasma were provided for compound exposure analyses.

Four volumes (w/v) of acetonitrile containing 0.1% formic acid was added to each tube containing hippocampal or cerebellar tissue. Samples were then homogenized using an ultrasonic probe and centrifuged using a benchtop centrifuge at 14,000 rpm for 20 min. Supernatant was diluted with sterile water and analyzed for nonlabled tracer concentration using LC/MS/MS. Standards were prepared by adding known quantities of the nonlabled tracer to brain tissue samples from non-treated rats and processing as described above.

Receptor occupancy was calculated using the ratio method (Chernet et al., 2005; Barth et al., 2006) using the following equation:

$$100*\{1-[(Ratio_t-1)/(Ratio_c-1)]\} = \%\ occupancy$$

Ratio refers to the ratio of nonlabled tracer concentration measured in the hippocampus (total binding region) to the nonlabled tracer concentration measured in the cerebellum (null binding region). $Ratio_t$ is the ratio determined in each animal treated with LY3130481 and $ratio_c$ is the average ratio in the vehicle treated animals.

2.8 *Quantitative PCR*

Quantitative PCR (qPCR) measured expression of TARPs, also known as calcium channel auxiliary gamma subunits, Cacng2 (TARP γ2), Cacng3 (TARP γ3), Cacng8 (TARP γ8), and Gria1 (GluA1) at mRNA level in cerebellum, lumbar of spinal cord, frontal cortex and hippocampus from male SD rats weighing 230-240 g and male CD-1 mice weighing 25-40 g. Total RNA was isolated from rat or mouse tissues using TRIzol reagent (Thermo Fisher Scientific/Invitrogen, Lenexa, KS). The isolated RNA was reversely converted to cDNA using SuperScript III kit (Thermo Fisher Scientific, Lenexa, KS). In brief, 2 µl of total RNA (250 ng/µl) was mixed with 10 µl of 2X Reaction mix, 2 µl of RT Enzyme and 6 µl of nuclease-free water. The reverse transcription reaction was conducted at 25°C for 10 min followed by 50°C for 30 min and 85°C for 5 min. After chilling on ice, 1 µl of RNase H was added into each reaction and the mixture was incubated at 37°C for 20 min. The cDNA was diluted four times with nuclease-free water. The qPCR reaction was performed by mixing 2.5 µl of diluted cDNA with 2 µl of Nuclease-free water, 5 µl of TaqMan gene expression master mix (Thermo Fisher Scientific/Applied Biosystems, Lenexa, KS) and 0.5 µl of qPCR primer/probe mix of each gene (Thermo Fisher Scientific/Applied Biosystems, Lenexa, KS, rat Hypoxanthine Phosphoribosyltransferase 1 (Hprt1), Rn01527840; rat Cacng2, Rn00584355; rat Cacng3, Rn00589900; rat Cacng8, Rn00589915, rat Gria1, Rn00709588; mouse Hprt1, Mm00446968; mouse Cacng2, Mm00432248; mouse Cacng3, Mm00517091; mouse

Cacng8, Mm00519222; mouse Gria1, Mm00433753). Data for each of the genes were replicated 3 times. The qPCR reaction was conducted with Quant Studio 7 Flex with pre-set relative qPCR program. The Ct value was calculated with a fixed threshold at 0.2 for all targets. ΔCt was calculated as $\Delta Ct = Ct_{gene} - Ct_{Hprt1}$. Data presented in graphs are relative expression to Hprt1 (or hippocampus), expressed as ΔΔCt ($\Delta\Delta Ct = \Delta Ct_{gene} - \Delta Ct_{normalizer\ (Hprt1\ or\ hippocampus)}$).

2.9 *In Vitro Electrophysiology*

Transfected Cell Preparation: The experimental procedure follows a previous report [20]. Briefly, human cDNAs encoding the flip-splice variant of GluA1 AMPA receptor principal subunits (GluA1i) (160 ng), TARP / CNIH-2 auxiliary subunits (40 ng), and a GFP (800 ng) driven by CMV promoter were mixed, and then incubated for 20 min with 100 µl of DMEM without serum or antibiotics containing 3 µl of Fugene 6 (Promega Biosciences, Madison, WI) for 25 min at room temperature. The plasmid DNA – Fugene 6 complex was added onto HEK 293T (1×10^6 cell/35 mm dish) cultured in DMEM + fetal bovine serum (10%) + penicillin / streptomycin (10 U/ml). When introducing multiple auxiliary subunit cDNAs into the cells at various ratios, we kept the total amount of the auxiliary subunit cDNAs at 40 ng. The cells were trypsinized one day after transfection and seeded on coverslips at 1:30 dilution to keep the cell density sparse enough to pick up single cells for the patch-clamp electrophysiological recording performed after over-night incubation. Electrophysiological recordings were performed after over-night incubation. To reduce the cytotoxicity by the AMPA receptor / auxiliary subunit expression, transfectants were cultured with NBQX (20 µM) until recording. Also, the transfection marker, a GFP-expressing plasmid was added at high ratio (80% weight of transfected DNA) compared to AMPA receptor / auxiliary subunit cDNAs.

Acutely Isolated Neuronal Preparations: This procedure is as previously described (Kato et al., 2016). Briefly, neurons were acutely isolated from cortical (ACC and SS), hippocampal, cerebellar, or spinal cord (dorsal half) taken from SD rats, CD1 or its congenic γ8 -/- mice (2-3 weeks postnatal). Tissue slices including the region(s) of interest were cut using a Vibroslice (Campden Instruments, London or

Leica, Milton Keynes, UK) in ice-cold slicing solution (concentrations in mM): NaCl 124, $NaHCO_3$ 26, KCl 3, glucose 10, $CaCl_2$ 0.5, $MgCl_2$ 4 with 300-305 mOsm and oxygenated with 95% O_2 and 5% CO_2. Slices were then incubated at 30–34°C in a modified carbogenated recording solution (concentrations in mM): NaCl 124, $NaHCO_3$ 26, KCl 3, glucose 10, $CaCl_2$ 2.3, $MgCl_2$ 1.3 with 300-305 mOsm for 30 min. The tissue was then incubated in a HEPES-buffered Hank's balanced salt solution containing protease 1 mg/ml Type XIV (Sigma-Aldrich, St. Louis, MO Aldrich) and maintained at 37° C with saturated 95% O_2, 5% CO_2. Following the incubation period, the brain regions were rinsed three times with trituration solution (concentrations in mM): Isethionic acid sodium salt 140, KCl 2, $MgCl_2$ 4.0, $CaCl_2$ 0.1, glucose 23, HEPES 15, pH 7.4, 300 mOsm, and cells were dissociated by trituration using fire-polished Pasteur pipettes. Hippocampal or cortical pyramidal neurons were identified by their triangle shape. Purkinje cells were identified by their large, round soma.

Tissue Slice Preparations: The brain or spinal cord was quickly removed and placed in an oxygenated, ice-cold beaker of slicing solution which contained (concentrations in mM): 110 NaCl; 10 $MgCl_2$; 2 KCl; 26 $NaHCO_3$; 1.25 NaH_2PO_4; 0.5 $CaCl_2$; 10 HEPES and 15 glucose (pH adjusted to 7.45 with NaOH, osmolarity was 308–312 mOsm, oxygenated with 95% O_2 and 5% CO_2). After cooling in slicing solution for 2–3 min, the whole brain or lumbar region of the spinal cord was blocked (portions of anterior and posterior tissue removed) using a razor blade and then glued to the microslicer tray using cyanoacrylate. (spinal cord was embedded in low gelling temperature agar). The tray containing the blocked and mounted tissue was filled with oxygenated, ice-cold slicing solution and serial, coronal sections were cut at a thickness of 300 µm. Once all slices were cut, they were placed in a larger recovery chamber containing oxygenated slicing solution at room temperature (18 to 20°C). The recovery chamber was in a large water bath which was initially at room temperature. Another slice keeper was placed into the water bath that contained aCSF composed of (in mM): 115 NaCl; 1.5 MgCl2; 4 KCl; 26 NaHCO3 ; 1.25 NaH2PO4; 10 HEPES; 1 CaCl2 and 15 glucose at pH 7.45, oxygenated with carbogen gas and osmolarity of 305 to 310 mOsm. The water bath was then turned on and the temperature was monitored inside the slice keeper. The recovery chamber temperature was allowed to reach 35 ± 0.4°C for a period

JPET Fast Forward. Published on March 25, 2019 as DOI: 10.1124/jpet.118.250126
This article has not been copyedited and formatted. The final version may differ from this version.

of approximately 30 minutes, after which the brain or spinal cord slices were transferred to the slice keeper containing the aCSF (which was at approximately the same temperature). Approximately 15 minutes after the slice transfer, the water bath was turned off and the slice keeper containing aCSF was allowed to slowly return to room temperature (18 to 20°C). Slices were used for recording after returning to approximately 32°C. The optimal total recovery time for the brain slices was approximately 2 to 2.5 hours.

Patch-clamp Recording: Electrophysiological recordings were made using boroscillicate glass electrodes having 2-5 MΩ resistances. For recordings from transfected cells or acutely isolated neuron, all cells were voltage-clamped at -80 mV and data were collected and digitized using Axoclamp 200B and Clampex software and hardware (Molecular Devices Inc., Sunnyvale, CA). For whole-cell recordings, the transfected HEK 293T cells were bathed in an external solution (concentrations in mM): NaCl 120.0, $BaCl_2$ 5.0, $MgCl_2$ 1.0, CsCl 20.0, glucose 10.0, HEPES 10.0; pH = 7.4 $\pm$ 0.3, containing 3-(2-Carboxypiperazin-4-yl)propyl-1-phosphonic acid (CPP) 0.1 and TTX 0.3 to block NMDA and voltage-dependent sodium channels, respectively. One of two electrode solutions were used (concentrations in mM): N-methyl-D glucamine160, $MgCl_2$ 4, Na-HEPES 40 pH 7.4, phosphocreatine12, Na_2-ATP 2.0, pH7.2 $\pm$ 0.02 adjusted by H_2SO_4, or (concentrations in mM) $CsMeSO_4$ 135, NaCl 8, HEPES 10,EGTA 0.3, Mg-ATP 4, Na-GTP 0.3. For some neuronal recordings, QX314 1 was added to the internal solution to block voltage-dependent sodium channels. The transfected HEK293T cell or the acutely isolated neuron was lifted and perfused with ligand-containing external solution from a sixteen-barrel glass capillary pipette array positioned 100-200 μm from the cells. Each gravity-driven perfusion barrel was connected to a syringe positioned approximately 30 cm above the recording chamber. The solutions were switched by sliding the pipette array with an exchange rate of less than 20 ms. Agonists and LY3130481 were applied where indicated.

The potency and efficacy of LY3130481 was calculated by measuring the amplitude $I_{Glu\ Steady\text{-}state}$ in the presence of LY3130481 normalized by $I_{Glu\ Steady\text{-}state}$ in the absence of LY3130481 to yield a relative

JPET Fast Forward. Published on March 25, 2019 as DOI: 10.1124/jpet.118.250126
This article has not been copyedited and formatted. The final version may differ from this version.

$I_{Glu\ Steady\text{-}state}$ value and plotted as a function of compound concentration (Log_{10}[LY3130481]). The average and SEM of $Log_{10}IC_{50}$ and efficacy (I_{max}) were calculated using the pooled Relative $I_{Glu\ Steady\text{-}state}$ values recorded from 3-6 cells using a three-parameter sigmoidal curve fitting function (Prism 7, GraphPad Software Inc.). For each cell, 5-6 concentrations of LY3130481 were applied. For curve-fitting purposes, a zero-drug value, i.e. Relative $I_{Glu\ Steady\text{-}state}$ without LY3130481 = 1, at [LY3130481] = 1×10^{-13} M, was included 3 log units below the lowest LY3130481 concentration tested. No constraints were applied to either the bottom or top values for curve fitting, so the calculated IC_{50} is relative IC_{50} and represents the concentration at the midpoint between the top and bottom plateau. The Hill coefficient (nH) was set to -1 because of the non-cooperative property of LY3130481.

For recordings from brain slices, tissue was placed in a superfusion chamber mounted on a Nikon Eclipse FN-1 microscope. Neurons within the region of interest were visualized using IR/DIC water immersion optics. The external solution contained (concentrations in mM): 115 NaCl; 1.5 $MgCl_2$; 5 KCl; 26 $NaHCO_3$; 1.25 NaH_2PO_4; 10 HEPES; 2 $CaCl_2$ and 15 glucose at pH 7.45, oxygenated with 95% O_2 and 5% CO_2 and osmolarity of 300–305 mOsm. The tissue slice in the chamber was continually superfused at a rate of 3 mL/min with oxygenated recording solution (18–20 °C). Compound containing solutions were applied to the slice via whole chamber superfusion. Glass recording electrodes were filled with (in mM): 130 K-gluconate; 5 NaCl; 2 $MgCl_2$; 10 HEPES; 2 MgATP; 0.2 NaGTP at pH 7.2 and osmolarity adjusted to 300 mOsm and had a resistance of 3 – 6 MΩ.

The whole-cell variant of the patch-clamp technique was used to record from visualized neurons and initial access resistance (Ra) was evaluated in voltage-clamp mode before switching to current clamp mode. Bipolar stimulating electrodes were placed near the recording electrode to evoke AMPA receptor-dependent excitatory postsynaptic potentials (EPSPs) from ACC neurons or on the attached dorsal root to elicit responses from spinal neurons in the superficial laminae of the dorsal horn. Constant current single stimulation pulses (100 μs, 50–500 μA) were delivered with a 20 s interstimulus interval. EPSPs were amplified with a Multiclamp 700B amplifier (Molecular Devices Inc., Sunnyvale, CA),

digitized and acquired using Clampex software (Version 10, Molecular Devices Inc., Sunnyvale, CA, Inc.). Once the EPSP was stable in recording solution only, slices were superfused with recording solution containing 10 μM bicuculline (bicuculline methochloride, Tocris 0130, mw = 440.37, batch 33A/124812), 50 μM APV (DL-APV, Tocris 0105, mw = 197.13, batch 28A/98113) and 1 μM strychnine (spinal cord slice only, Sigma S8753, mw = 370.87) to block the GABA, NMDA and Glycine (in spinal cord slice) components of the EPSP, respectively, leaving only the AMPA mediated EPSP. Once the AMPA mediated EPSP was stable, a single concentration (300 nM, or 3 μM) of the TDAA 3130481 (mw = 382.44, ref. L37-H71437-028) dissolved in recording solution containing bicuculline, strychnine and APV, was superfused over the slice for 60 minutes. At the end of the 3130481 exposure period the non-TARP dependent AMPA antagonist, GYKI 53784 (303070, mw = 352.39, ref. MN3-E07803-030) was applied at 50 μM to show that the EPSP was completely AMPA mediated. Due to the extended time of the exposure to 3130481 during the experiment a separate series of experiments were performed in order to determine the effect of time on the magnitude of the electrically evoked EPSP in which all solutions were the same except 3130481 was absent. The bicuculline/APV/strychnine solution and all compound containing solutions contained 0.1 to 0.2% DMSO.

The data from these experiments was analyzed in two different ways. First, the peak amplitude of the EPSPs was measured for the entire experimental duration. The EPSP amplitude as plotted against time and an exponential smoothing algorithm was used to smooth the trending line of the plot. The smoothed data was then converted to a percentage of the experimental baseline time period average and then individual experiment time points were averaged and SEMs determined. In the second analysis method the EPSP traces were analyzed for peak amplitude values by averaging at least five traces at the end of each treatment period and then converting that average value to a percentage of the experimental baseline time point. All parameters were analyzed using Clampfit v10 and data were compiled and summarized (means and SEMs calculated) using Excel. Plotting of the data and statistical analysis of the processed data was performed using GraphPad Prism 7.

2.10 *In Vivo Electrophysiology*

Male SD rats (Harlan, Indianapolis, IN, USA) (200-240 g) were utilized. Electrophysiological recordings were performed in rats anesthetized with 1.5 g/kg of urethane. Catheters were inserted into the jugular vein and carotid artery, to administer drugs and monitor blood pressure, respectively. Mean arterial blood pressure was monitored continuously and was maintained at >80 mmHg, and body temperature was maintained at 37ºC using a thermoprobe. Rats were mounted in a stereotaxic apparatus, and the lumbar enlargement was exposed via laminectomy (T12-L3). Following removal of the dura, the exposed spinal cord was kept moist with a small amount of artificial cerebrospinal fluid. A tungsten microelectrode (1MΩ, FHC, Bowdoinham, ME) was inserted into the spinal cord at level L4–L5 and advanced using a microdrive system (Burleigh, Fisher, NY) in 10 μm increments. Once a single-unit was isolated from background activity, the action potentials were monitored continuously by an analog signal delay unit and displayed on a storage oscilloscope after initial amplification through a low-noise AC differential amplifier. The electrophysiological activity was processed through a window discriminator and counted using the Spike2/CED 1401 data acquisition program (Cambridge Electronic Design Ltd., Cambridge, England). Single spinal dorsal horn sensory neurons were identified by brushing and mild pinching of the hind paw, and the receptive fields located on the plantar surface of the hind paw were then mapped using von Frey filaments. Only wide dynamic range (WDR) neurons were recorded in the present study. After a WDR neuron was identified, a pair of fine needles was inserted into the receptive field to deliver electrical stimulation. The threshold for action potential generation was determined by delivering single electrical pulses (2 ms duration) of increasing intensity. Wind up of WDR spike discharge was evoked by delivering a train of stimulation pulses (16 pulses in 32 s, 0.5 Hz, 2 ms duration). Control responses were determined as the average of two consistent responses 10 min apart to stimulation of the receptive field. Wind-up discharge was calculated using methods similar to those described previously (Bee and Dickenson, 2009). The input value was defined as number of action potentials evoked by the first of 16 stimulation pulses. The wind-up response was calculated by measuring the total cumulative number of action potential discharges evoked by the 16

stimulation pulses minus the input value. The effects of i.v. administration of vehicle, LY3130481 (1, 3, 10 mg/kg cumulative dosing) or GYKI52466 (6 mg/kg) on the wind-up discharge of WDR spinal sensory neurons were evaluated. Electrical stimulation pulses were delivered every 10 min to yield data points for 10 and 20 min post drug. At the conclusion of the experiments, rats were euthanized with urethane followed by cervical dislocation.

2.11 *Autoradiography*

Cohorts of $\gamma8^{-/-}$ mice were obtained from Prof. Roger Nicoll (Unversity of California, San Francisco) and bred at a contract breeder (Taconic, Cambridge City, IN, USA). A detailed description of the generation of the $\gamma8^{-/-}$ mouse line was published by Rouach et al. (2005). For these experiments, male $\gamma8^{+/+}$ and $\gamma8^{-/-}$ mice weighing 25-30 g were sacrificed by rapid decapitation and their brains quickly removed and frozen on dry ice. On the day of sectioning, frozen tissue was mounted on cryostat chucks and equilibrated to cryostat temperature of -20º C (object temperature approximately -16º C). Frozen sections of 12 µm were cut and thaw-mounted on gelatin-coated slides. Sections were allowed to dry at room temperature and then stored at -80º C in sealed containers. Slide-mounted tissue sections were thawed to room temperature before removal from the sealed containers, labeled with a scriber pen, pre-incubated at room temperature in assay buffer for 15 min to remove endogenous receptor ligands, and then dried completely under a stream of cool air. Sections were incubated on ice for 2 hrs in 20 mM HEPES, 400 mM NaCl and 10 mM MgCl containing 3 nM [^{3}H]-LY3074158, which corresponds to [^{3}H]-compound **3** in our previous report (Lee et al., 2017), with and without 10 µM LY3187358 for nonspecific binding. Following incubation, the sections were rinsed twice by immersing in ice-cold assay buffer for 5 min, followed by a final quick rinse in ice-cold purified water, then dried under a stream of warm air. Slides were placed in film cassettes with Fuji BAS-TR2025 phosphoimaging plates and exposed for an empirically determined duration. Radioactive standards calibrated with known amounts of [^{3}H] (American Radiolabelled Chemicals, Inc. ARC-0123), were co-exposed with each plate. Autoradiogram analysis was performed using a computer-assisted image analyzer (MCID7.0; Imaging

Research Inc., St. Catherines, Ontario). Images were colorized using the MCID software, and stored as TIFF files.

2.12 *Membrane Microtransplantation into Xenopus Oocytes*

Frozen samples of human spinal cord, cortex and cerebellum were obtained from Tissue Solutions (Clydebank, Scotland) and Analytical Biological Services Inc. (Wilmington, Delaware, U.S.A.). Samples were from control donors. Brain samples were kept frozen at -80°C and transport of the samples took place on dry ice. Membrane preparations from these tissues were prepared according to the method developed and described by (Miledi et al., 2002; Miledi et al., 2006; Eusebi et al., 2009; Kato et al., 2016). In short, 0.1–0.5 g of tissue was homogenized in ice-cold glycine buffer (concentrations in mM: 200 glycine, 150 NaCl, 50 EGTA, 50 EDTA, 300 sucrose) to which 10 μL protease inhibitor cocktail (Sigma-Aldrich, St. Louis, MO) was added per ml glycine buffer. The homogenate was centrifuged at 4°C for 15 min at 9500 g. The supernatant was subsequently centrifuged at 4°C for 2 hr at 100,000 g with an ultra-centrifuge and the pellet was re-suspended in ice-cold assay buffer (5 mM glycine). The protein concentration of the membrane preparations was measured using the Pierce BCA protein assay kit (Thermo Scientific, Rockford, IL, USA) and was ~3 mg/ml. Aliquots of the suspensions were kept at -80°C and were thawed just before injection into Xenopus oocytes.

Xenopus oocytes (stage V-VI) were removed from schedule I sacrificed frogs and defolliculated after treatment with collagenase type I (5 mg/ml calcium-free Barth's solution) for 4 h at room temperature. 60 nl of membrane suspension was injected per oocyte using a Drummond variable volume microinjector (Broomall, PA, U.S.A.). After injection, oocytes were incubated at 18°C in a modified Barth's solution containing (concentrations in mM): NaCl 88, KCl 1, $NaHCO_3$ 2.4, $Ca(NO_3)_2$ 0.3, $CaCl_2$ 0.41, $MgSO_4$ 0.82 , HEPES 15 and 50 mg/l neomycin (pH 7.6 with NaOH; osmolarity 235 mOsm). Experiments were performed on oocytes after 2-5 days of incubation.

Oocytes were placed in a recording chamber (internal diameter 3 mm), which was continuously perfused with a saline solution (concentrations in mM): NaCl 115, KCl 2.5, $CaCl_2$ 1.8, $MgCl_2$ 1, HEPES

10, pH 7.3 with NaOH, 235 mOsm) at a rate of approximately 10 ml/min. Dilutions of drugs in external saline were prepared immediately before the experiments and applied by switching between control and drug-containing saline using a BPS-8 solution exchange system (ALA Scientific Inc., Westbury, NY, U.S.A.). Oocytes were impaled by two microelectrodes filled with 3 M KCl (0.5 – 2.5 MΩ) and voltage-clamped using a Geneclamp 500B amplifier (Axon Instruments, Union City, CA, U.S.A.). The external saline was clamped at ground potential by means of a virtual ground circuit using an Ag/AgCl reference electrode and a Pt/Ir current-passing electrode. The membrane potential was held at -60 mV. The current needed to keep the oocyte's membrane at the holding potential was measured. Membrane currents were low-pass filtered (four-pole low-pass Bessel filter, -3 dB at 10 Hz), digitized (50 Hz), and stored on disc for offline computer analysis. Data are expressed as mean ± SEM. Experiments were performed at room temperature.

For the inhibition curve, currents were evoked by switching from control solution to a solution containing 100 μM AMPA and 30 μM cyclothiazide (CTZ). After 5 min of AMPA/CTZ perfusion the solution was switched to AMPA/CTZ plus various concentrations of LY3130481 for 5 min. The amount of inhibition was calculated from the current amplitude at the end of LY3130481 application and the current amplitude of the AMPA/CTZ response just before LY3130481 application.

The concentration-inhibition curve was fitted according to the Hill equation. Curve fitting was performed using Graphpad Prism 3.01 software (San Diego, CA, USA).

3. Results

3.1 *Recombinant AMPA Receptors*

Previous studies have found that LY3130481 potently and selectivity blocks AMPA receptors containing γ8 subunits compared to AMPA receptors associated with other TARPs or without auxiliary proteins (Gardinier et al., 2016; Kato et al., 2016). This γ8-specificity is not dependent on GluA subunit subtype (1-4), heteromeric configurations, or splice variation (Kato et al., 2016). Here, we extend these

findings by examining the effects of varying the transfection ratios of γ8 with other TARPs that are predominantly expressed in spinal (γ2) and cortical neurons (γ3) involved in pain signaling. The effects of LY3130481 were evaluated on HEK cells heterologously expressing GluA1i and γ8 alone or in combination with different ratios of γ8 and γ2 or γ3. Results showed that LY3130481 (0.001-30 μM) had no appreciable effect on the glutamate-evoked (1 mM) responses of GluA1i receptors expressed alone that were marked by a fast inward current that rapidly desensitized to a small steady-state level (Fig. 1A). Co-expression with any of the TARP subunits increased the amplitude of the glutamate-evoked desensitized current, and for γ8-containing receptors, the current displayed a unique response characterized by a gradual increase in amplitude associated with prolonged glutamate application (Kato et al., 2010) (Fig. 1A and Supplemental Fig. 1). This response has previously been described as "resensitization" (Kato et al., 2010; Gill et al., 2011; Gill et al., 2012), although the mechanism is not known. Consistent with prior reports (Gardinier et al., 2016; Kato et al., 2016; Lee et al., 2017) , LY3130481 potently and selectively blocked γ8-containing GluA1i receptors with an IC_{50} of 6.6 nM, (*n*=5), while having minimal to no effect on GluA1i receptors co-expressed with γ2 or γ3 subunits or CNIH-2 (Fig. 1 Supplemental Fig.1 and Supplemental Table 1) up to a concentration of 10 μM. The γ8-selectivity of LY3130481 contrasted with the effects of the non-selective AMPA antagonist, GYKI52466 which was equally potent and efficacious at blocking glutamate-evoked currents from γ2- (*n*=5) or γ8-containing (*n*=4) AMPA receptors (Fig. 2A, B and Supplemental Table 2). As well, co-transfection of γ2 with γ8 at a ratio of 1:1 or 10:1 (*n*=5) had no effect on the activity of GYKI52466 relative to that of either transfectant alone (Fig. 2A, B and Supplemental Table 2).

Additional studies previously have demonstrated that LY3130481 has minimal to no effect as either an antagonist or positive allosteric modulator on related ionotropic glutamate receptors, including GluK2, GluN1/GluN2A, GluN1/GluN2B or metabotropic glutamate receptors (mGluR), mGluR1,2,3,4,5 and 8 (Kato et al., 2016). Moreover, LY3130481 does not have appreciable binding to 19 additional

targets, including neurotransmitter receptors, ion channels and transporters (Kato et al., 2016). Taken together, these data demonstrate that LY3130481 is highly selective for γ8-containing AMPA receptors.

The effect of modifying TARP transfection ratios was next evaluated by co-transfecting GluA1i with different ratios of cDNAs encoding γ8 and γ2 or γ3. Varying the γ2:γ8 ratio from 0:1 to 10:1 produced a marked decrease in the potency and maximal efficacy (as measured at 10 μM) of LY3130481 in blocking glutamate-evoked currents (Fig. 1A, B and Supplemental Table1). The potency decreased by ~270-fold from an IC_{50} of 6.6 nM (γ8 alone) to 1800 (*n*=6) nM (10:1) and the maximal efficacy was reduced from >90% to ~50% (Fig. 1B and Supplemental Table 1). Co-transfection of γ2 and γ8 cDNAs at different ratios with GluA1i produced an attenuation of the resensitization of inward current in response to prolonged glutamate application. Indeed, even a γ2:γ8 ratio of 1:3 effectively suppressed resensitization despite having modest effects on the potency and efficacy of LY3130481 (Fig. 1A, B and Supplemental Fig. 1A). When potency and efficacy were plotted as a function of the percentage of resensitization, results showed that most of the γ2/γ8 co-transfectants displayed no resenstization, but were potently and efficaciously blocked by LY3130481 (Supplemental Fig. 1A). These data suggest that γ2 and γ8TARPs can co-assemble into functional AMPA receptors which display a range of sensitivity to LY3130481 that is dependent on the relative transfection stoichiometries of the two subunits.

Although altering the ratio of γ3: γ8 also decreased the potency and maximal efficacy of LY3130481 on GluA1i currents, the magnitude of these shifts was significantly smaller than for γ2 co-transfectants. For example, a ratio of γ3:γ8 of 10:1 shifted the potency of LY3130481 by approximately 7-fold (IC_{50} = 42 nM, *n*=6) compared to γ8 alone and the efficacy was reduced to 72.8 % (*n*=6) (Fig. 1A, C and Supplemental Table 1). Similar to γ2 co-transfectants, γ3 suppressed the resensitization response of γ8-containing GluA1i receptors in a steeply ratio-dependent manner, indicating that γ3 subunits can co-assemble with γ8 into functional receptors having a range of responses to LY3130481 (Fig. 1A, Supplemental Fig 1B). The attenuation of γ8-dependent

JPET Fast Forward. Published on March 25, 2019 as DOI: 10.1124/jpet.118.250126
This article has not been copyedited and formatted. The final version may differ from this version.

resensitization by co-transfection with γ2 or γ3 is reminiscent of that with CNIH-2 (Supplemental Fig. 1C) (Kato et al., 2010). Thus, while shifts in potency and maximal efficacy of LY3130481 on GluA1i currents were dependent on the ratio of co-transfection of these other auxiliary subunits with γ8, the magnitude of the shifts were greatest when γ2 was combined with γ8.

The effect of TARP transfection ratios on the potency and efficacy of LY3130481 was also evident on putative heteromeric receptor complexes. For example, LY3130481 was highly potent and efficacious in suppressing glutamate-evoked currents from cells co-transfected with γ8 in combination with GluA1i and GluA2i (Supplemental Fig.2A, B and Supplemental Table 3). In GluA1i/GluA2i-containing cells, γ8 expression produced a resensitization of the glutamate-evoked response. Similar to GluA1i receptors, co-transfection of γ2 and γ8 in increasing ratios in GluA1i/GluA2i-containing cells blocked resensitization and markedly shifted the potency and efficacy of LY3130481 (Supplemental Fig. 2A, B, Supplemental Table 3). Additional studies showed that although the potency and efficacy of LY3130481 were reduced in cells co-transfected with γ8 and GluA2i and GluA3i compared to homomeric GluA1i or GluA1i/GluA2i-containing cells (Supplemental Fig. 2C, D), similar shifts of LY3130481 activity were observed with co-transfection of γ2 and γ8 in increasing ratios in GluA2i/GluA3i-containing cells (Supplemental Fig. 2D and Supplemental Table 4).

3.2 *Native AMPA Receptors*

The alterations in potency and efficacy of LY3130481 produced by varying the transfection ratio of γ8 with other auxiliary subunits suggests that the compound will differentially affect native AMPA receptors in CNS neurons, depending on their levels of γ8 expression. Initial studies investigated the relative expression of mRNA for γ2, γ3 and γ8 TARPs and the GluA1 subunit quantified by RT-qPCR in samples from in frontal cortex, hippocampus, cerebellum and spinal cord of rats. Consistent with previous reports (Tomita et al., 2003), γ2, γ3 and γ8 expression were highest in cerebellum, frontal cortex and

hippocampus, respectively (Fig. 3A-D). Within spinal cord, γ8 and γ2 mRNAs were expressed at relatively low levels, but higher than γ3 mRNA. In frontal cortex, γ8 mRNA abundance was greater than γ3 and γ2 expression. The mRNA GluA1 subunit had a rank order of expression from highest to lowest in hippocampus, cerebellum, frontal cortex and spinal cord by qPCR (data not shown).

The relative expression of γ2, γ3 and γ8 mRNA in hippocampus, frontal cortex, cerebellum and spinal cord found in the present studies is consistent with the heterogeneous protein expression levels of these subunits in brain and spinal cord described previously (Larsson M, 2013; Sullivan SJ, 2017). With respect to the expression of these TARPs in spinal cord, the modest levels of γ8 mRNA were somewhat unexpected given the previous immunohistochemical studies (Larsson M, 2013) though see Sullivan et al. (Sullivan SJ, 2017). To clarify the distribution of γ8 binding sites in brain and spinal cord, we leveraged a radiolabeled version [^{3}H]-LY3074158 (Compound **3** in (Lee et al., 2017), a close congener of LY3130481. In functional assays examining glutamate-stimulated calcium flux, LY3074158 was inactive at GluA1i receptors alone or co-expressed with γ2, but highly potent at blocking GluA1i receptors co-expressed with γ8 (IC_{50} = 15.7 ± 10.2 nM, *n*=30 mean ± SEM). In addition, [^{3}H]-LY3074158 displayed high affinity (K_D=4 nM) for hippocampal AMPA receptors in binding assays. Together, these data confirm the potency and selectivity of LY3074158 for recombinant and native γ8-associated AMPA receptors.

Autoradiograms were generated showing total binding of [^{3}H]-LY3074158 in tissue slices from brain and spinal cord of $\gamma8^{+/+}$ and $\gamma8^{-/-}$ mice. Consistent with the present qPCR results and previous *in situ* hybridization, immunohistochemical and radio-ligand binding studies (Tomita et al., 2003; Lee et al., 2017; Sullivan SJ, 2017), [^{3}H]-LY3074158 binding was highest in hippocampus, moderate in cortex, lower in spinal cord and at background levels in cerebellum (Fig. 3 E-H, K). The γ8-specific binding of [^{3}H]-LY3074158 was determined from autoradiograms from $\gamma8^{-/-}$ mice and revealed a large reduction in hippocampus and a smaller, but significant reduction in spinal cord, consistent with expected levels of

JPET Fast Forward. Published on March 25, 2019 as DOI: 10.1124/jpet.118.250126
This article has not been copyedited and formatted. The final version may differ from this version.

γ8 protein expression (Fig. 3K). For comparison, the relative γ8 mRNA expression from *in situ* hybridization studies (Allen Brain Atlas (Lein et al., 2007)) is presented in Fig. 3 I,J.

The functional consequences of the heterogeneous expression of TARPs were next investigated on neurons isolated from four distinct CNS regions. In agreement with previous studies (Kato et al., 2016), the potency and efficacy of LY3130481 were greatest on AMPA responses from acutely isolated hippocampal pyramidal neurons (IC_{50} = 27 nM, I_{max} = 85%, *n*=3) (Fig. 4 A, B, Supplemental Table 3) which display the highest levels of γ8 expression (Tomita et al., 2003) and [^{3}H]-LY3074158 binding in brain and were very similar to the potency and efficacy profiles of LY3130481 found for cells recombinantly co-expressing GluA1 with γ8 (Fig. 1B, Supplemental Table 1). In contrast, LY3130481 had almost no effect on AMPA responses in isolated cerebellar Purkinje neurons (*n*=3) which have high γ2, but low γ8 expression (Tomita et al., 2003) similar to cells recombinantly co-expressing GluA1i and γ2 (Fig. 4 A and Supplemental Tables 1 and 5). Consistent with the more modest expression of γ8 and equivalent expression of γ2 in spinal cord, the activity of LY3130481 on AMPA responses in these cells was considerably less potent (IC_{50} = 7.7 μM, *n*=6) (Fig. 4, Supplemental Table 5) and similar to the responses of recombinant cells expressing higher ratios of γ2:γ8 (i.e., 10:1) (Fig. 1B and Supplemental Table 1). In comparison to spinal neurons, the effects of LY3130481 on isolated pyramidal neurons from ACC (IC_{50} = 46 nM, I_{max} = 65.6%, *n*=3) and SS (IC_{50} = 52 nM, I_{max} = 65%, *n*=5) cortices were more potent and efficacious (Fig. 4 A and Supplemental Table 5). As well, the activity of LY3130481 on these neurons was in agreement with the relative expression of γ8 and the γ3 in cortical regions and the more modest alterations in potency and efficacy conferred by recombinantly expressed γ8 and γ3 in stoichiometric studies (Fig. 1C, Supplemental Table 1). In contrast to the differential effects of LY3130481 on native receptors, GYKI52466 was equally potent and efficacious on hippocampal and ACC pyramidal neurons and cerebellar Purkinje cells (Fig. 2C and Supplemental Table 6).

The γ8-dependence of LY3130481 activity on neuronal AMPA receptors was evaluated using isolated neurons from $\gamma8^{+/+}$ and $\gamma8^{-/-}$ mice. Initial studies showed that the potency and efficacy of LY3130481 on

JPET Fast Forward. Published on March 25, 2019 as DOI: 10.1124/jpet.118.250126
This article has not been copyedited and formatted. The final version may differ from this version.

hippocampal (IC_{50} = 26 nM, I_{max} = 88%, *n*=3) and ACC (IC_{50} = 46 nM, I_{max} = 68%, *n*=3) neurons from $\gamma8^{+/+}$ mice were very similar to values found for these cell types harvested from rat brains (Fig. 4B, Supplemental Table 7). In contrast, the effect of LY3130481 on hippocampal neurons from $\gamma8^{-/-}$ mice was abolished up to concentrations of 30 μM and the potency was reduced by nearly 200-fold in ACC neurons (IC_{50} = 8.5 μM, *n*=4) (Fig. 4B, Supplemental Table 7). Interestingly, the concentration-response profile of LY3130481 on ACC neurons from $\gamma8^{-/-}$ mice closely resembled the profile observed in cells recombinantly co-expressing GluA1i and γ3 (see Fig. 1C) and is consistent with the presence of γ3 in ACC. Taken together, these data demonstrate the γ8-dependence of LY3130481 on the native neuronal AMPA receptors.

The relevance of LY3130481 activity in rodent tissue to that from humans was next assessed on AMPA receptors reconstituted from human cortex, spinal cord and cerebellum into Xenopus oocytes in a manner similar to that previously reported for human hippocampus and cerebellum (Kato et al., 2016). LY3130481 suppressed AMPA receptor-mediated currents from heterologously-expressed cortical AMPA receptors in a concentration-dependent manner with high potency (IC_{50} = 53 nM) and efficacy (I_{max} ~ 85%) similar to that for rodent cortical neurons (Fig. 4A and Fig. 5 A, B). Responses of reconstituted human spinal AMPA receptor responses were reduced by LY3130481 albeit with a lower potency (IC_{50} = 485 nM) and partial efficacy (I_{max} = 57%) similar to effects on AMPA receptors in acutely-isolated rodent spinal neurons (Fig. 4A and Fig. 5C, D). By comparison, LY3130481 minimally suppressed AMPA receptor-mediated currents from reconstituted human cerebellar tissue (Fig. 5E). Collectively, these studies on indicate that the differential effects of LY3130481 on distinct neuronal populations are predicted by the regional expression of γ8, γ2 and γ3 in rodent and human brain.

3.3 *Modulation of Synaptic Transmission*

The partial blockade of AMPA responses of isolated spinal and cortical neurons suggested that the compound should display a similar reduction of AMPA receptor-mediated synaptic responses in these two CNS regions, albeit with different potencies. To test this hypothesis, the glutamatergic synaptic

responses of ACC pyramidal neurons were evoked by stimulation of fibers in the proximal apical dendritic region of these neurons in a tissue slice preparation. Because of the dense recurrent excitatory collateral network among cortical neurons, the synaptic response is composed of both mono- and polysynaptic components, yielding a complex EPSP (Baumbarger et al., 2001). The AMPA receptor-mediated component of the synaptic response was isolated by blocking $GABA_A$ and $GABA_B$ receptors and NMDA receptors with bicuculline (1 μM), SCH50911 (2 μM), and APV (50 μM), respectively. Previous studies examining the effects of LY3130481 on synaptic transmission in hippocampal slices have shown that the drug requires approximately 30 min to reach a steady-state level (Kato et al., 2016). To evaluate the potential confound of a decrement in ACC responses associated with long exposure times, initial studies measured the amplitude of the ACC EPSP over time and demonstrated that the responses were stable for at least 70 min (Fig. 6 A). Subsequent experiments demonstrated that 0.03 μM and 0.3 μM LY3130481 reduced the AMPA receptor-dependent EPSP in ACC neurons to 35.8 ± 5.2 % and 41.8 ± 2.7% (*n*=4) of control responses, respectively (Fig. 6 A, B). In contrast, the non-selective AMPA receptor antagonist, GYKI53784 (50 μM) abolished the AMPA receptor-mediated responses of ACC neurons (Fig. 6 B).

The effects of LY3130481 were also studied on the AMPA receptor-mediated synaptic transmission in spinal dorsal horn neurons evoked by stimulation of dorsal roots. Results showed that 0.03 μM and 0.3 μM LY3130481 suppressed responses of spinal neurons in a concentration-dependent manner, to 87.6 ± 3.8% and 53.9 ± 1.7% (*n*=4) of control responses (Fig.6 C, D). Time control experiments demonstrated that the amplitude of the synaptic response of dorsal horn neurons was stable for at least 70 min, indicating that the effects of LY3130481 were not likely due to deterioration of the recording. Similar to its effects on synaptic responses of ACC neurons, GYKI53784 (50 μM) completely blocked the EPSP in spinal neurons (Fig. 6 D). Collectively, these data support the hypothesis that potency and efficacy of LY3130481 on AMPA receptor-mediated synaptic transmission in different CNS neurons depend on the relative abundance of the γ8 subunit.

JPET Fast Forward. Published on March 25, 2019 as DOI: 10.1124/jpet.118.250126
This article has not been copyedited and formatted. The final version may differ from this version.

3.4 *Pharmacokinetics and Receptor Occupancy*

To inform in vivo studies, the pharmacokinetic properties and CNS receptor occupancy characteristics of LY3130481 were assessed. Plasma concentration-time profiles following p.o. (3 mg/kg) and i.v. (1 mg/kg) administration in rat showed LY3130481 had high oral bioavailability (97%) (Fig. 7 A). Oral dosing delivered compound to plasma with a C_{max} of 628 ng/mL (1.6 μM), T_{max} of 1.3 hr and half-life of 2.4 hr. The clearance of LY3130481 (Cl = 11 mL/min-kg) was relatively low compared to hepatic blood flow (Qh = 55 mL/in-kg) and contributed to the high oral bioavailability. The occupancy of γ8-containing AMPA receptors in brain was measured following oral administration of LY3130481 (0.1-30 mg/kg) using a pre-treatment time of 1 hr. LY3130481 displayed a dose-dependent increase in plasma concentration that was correlated with CNS γ8-AMPA receptor occupancy. Inspection of the dose-occupancy relationship showed that LY3130481 had an ED_{50} of 2.9 mg/kg (*n*=4, pooled data) and a maximal efficacy of 96% occupancy at 30 mg/kg (Fig. 7 B). These data were used to guide dosing for subsequent in vivo PD assessments.

3.5 *Modulation of Synaptic Plasticity*

A role for AMPA and N-methyl-D-aspartate (NMDA) receptors in the short-term enhanced responsiveness of spinal sensory neurons to repetitive c-fiber stimulation (i.e., wind-up) and the induction of long-term increases in spinal neuron excitability (i.e., central sensitization) produced by stimulation or peripheral nerve injury is well-established (Davies SN, 1987; Dickenson and Sullivan, 1987; Dickenson, 1990; Svendsen et al., 1998; Herrero et al., 2000). Non-selective blockade of AMPA receptors prevents the induction of both forms of synaptic plasticity, as well as suppresses the expression of previously established sensory neuron hyperexcitability (Dickenson and Sullivan, 1987; Dickenson, 1990; Svendsen et al., 1998; Herrero et al., 2000). Given the effects of LY3130481 on AMPA receptor-dependent synaptic responses of spinal neurons in vitro, the present studies tested the hypothesis that selective blockade of γ8-containing AMPA receptors could also attenuate wind-up of spinal sensory neurons to c-fiber stimulation in vivo. Consistent with previous studies (Davies SN,

JPET Fast Forward. Published on March 25, 2019 as DOI: 10.1124/jpet.118.250126
This article has not been copyedited and formatted. The final version may differ from this version.

1987; Dickenson and Sullivan, 1987), repetitive stimulation of peripheral nerves evoked an increase in discharge of single wide-dynamic range (WDR) neurons to successive stimuli (i.e., wind-up) (Fig. 8 A). Intravenous delivery of the vehicle solution did not affect the wind-up discharge of WDR neurons (105.1 ± 7.8%, *n*=8 of pre-treatment). However, administration of cumulative doses (1, 3, 10 mg/kg, i.v.) of LY3130481 produced a dose-dependent decrease in wind-up discharge of c-fiber inputs to WDR neurons (Fig. 8 A, B). Wind-up responses were significantly, but only partially reduced to 74.8 ± 6.2% (*n*=8), 66.3 ± 7.0% (*n*=8) and 56.6 ± 7.3% (*n*=7) of control values following administration of 1, 3 and 10 mg/kg doses, respectively (Fig. 8 B). In comparison, systemic administration of the non-selective AMPA receptor antagonist, GYKI52466 (6 mg/kg) suppressed wind-up discharge to 28.2 ± 9.2% (*n*=4) of control values (Fig. 8 B), significantly greater than the highest dose of LY3130481 (10 mg/kg). The suppressive effects of LY3130481 also were evident in the discharge to the initial stimulus in the repetitive train in the wind-up studies. LY3130481 reduced discharge to the first stimulus in the repetitive train to 62.8 ± 6.5% (*n*=8), 60.9 ± 10.2% (*n*=7), and 44.0 + 10.9% (*n*=7), of control values following administration of 1, 3 and 10 mg/kg doses, respectively. GYKI52466 (6 mg/kg) also reduced discharge to the initial stimulus to 33.4 ± 6.5% (*n*=5) of control responses (Fig. 8 C).

Due to the cumulative dosing paradigm, plasma exposure of LY3130481 was not measured in these animals. Rather, in a separate experiment, animals were dosed intravenously with either 1 mg/kg or 10 mg/kg of LY3130481 and sample analyses yielded LY3130481 plasma levels (concentrations) of 1140 ± 177 ng/mL (*n*=3) (3 μM) and 11485 ± 857 ng/mL (*n*=7) (30 μM), respectively. Examination of the exposure-occupancy curve for LY3130481 indicates that these plasma concentrations are predicted to be associated with CNS γ8-AMPA receptor occupancy levels of ~50% and 100%, respectively (Fig. 8 B). These data demonstrate that LY3130481 reduced glutamatergic synaptic transmission and short-term synaptic plasticity of c-fiber inputs to spinal sensory neurons *in vivo*. However, the suppression of excitatory responses was only partial despite near-complete occupancy of CNS γ8-AMPA receptors, suggesting that only a sub-population of synaptic AMPA receptors on WDR neurons contain the γ8 subunit.

3.6 *Attenuation of Nocifensive Behavior*

Modulation of the nocifensive behaviors of conscious animals in response to noxious stimuli, tissue injury or nerve damage has been used extensively to evaluate the therapeutic potential of novel agents. Intraplantar injection of formalin has been shown to initiate dramatic increases in spontaneous activity of c-fibers and discharge of WDR neurons in the spinal cord and ACC and SS cortical neurons (Chapman and Dickenson, 1995; McCall et al., 1996). Coupled with these excitatory responses, animals exhibit a unique behavioral response to formalin characterized by an initial bout of nocifensive responding that subsides approximately 5-10 min after formalin injection, followed by a longer period of responding lasting approximately 45-60 min. This behavioral response pattern is associated with an analogous pattern of discharge of WDR neurons with both indices being dependent on enhanced glutamatergic synaptic input (Haley et al., 1990; Coderre and Melzack, 1992; Hunter JC, 1994). Previous studies have demonstrated that the formalin-induced nocifensive behavior can be reduced by systemic administration of broad-spectrum AMPA receptor antagonists, albeit with significant motor and sedative side-effects (Simmons RM, 1998) . The present studies tested the hypothesis that selective blockade of γ8-containing AMPA receptors would suppress formalin-induced behaviors without confounding CNS side-effects. Indeed, oral administration of LY3130481 attenuated formalin-induced nocifensive behaviors in both Sprague Dawley rats (Fig. 9 A) and CD-1 mice (Fig. 10 A) in a dose-dependent manner. The ED_{50} values of LY3130481 in both species were comparable (rat = 3.7 mg/kg, mice = 4.7 mg/kg) and the decrease in nocifensive behaviors was observed in the absence of any overt impairment as measured by rotorod performance (Fig. 10 C). In contrast, although GYKI52466 also dose-dependently suppressed nocifensive behaviors in the mouse formalin assay, marked impairment on rotorod performance was observed in an overlapping dose range (Fig. 10 B, D). These data are consistent with previous reports on global AMPA antagonists (Simmons RM, 1998).

Further support for a role of γ8-containing AMPA receptors in the anti-nocifensive effects of LY3130481 came from an examination of the dose-occupancy and dose-response relationships in rats

JPET Fast Forward. Published on March 25, 2019 as DOI: 10.1124/jpet.118.250126
This article has not been copyedited and formatted. The final version may differ from this version.

for LY3130481 in CNS γ8-AMPA receptor occupancy and formalin assays, respectively. The data revealed that the dose-dependent increase in CNS receptor occupancy was inversely related to nocifensive responding in the late phase of the formalin response (Fig. 9 B). Indeed, the potency for occupancy of CNS γ8-containing AMPA receptors (ED_{50} = 2.9 mg/kg) was nearly identical to the potency for attenuation of formalin-induced behaviors (ED_{50} = 3.7 mg/kg).

The γ8-dependence of the anti-nocifensive actions of LY3130481 were subsequently explored using $\gamma8^{+/+}$ and $\gamma8^{-/-}$ mice. Initial studies showed that $\gamma8^{-/-}$ mice had similar levels of responding to formalin injection compared to $\gamma8^{+/+}$ mice (Fig. 11 A). This may reflect compensation mechanisms in response to the loss of the gene throughout development, allowing alternative mechanisms to underlie the formalin-induced behavior. When LY3130481 was administered at the ED_{50} dose, nocifensive behavior was present in the $\gamma8^{+/+}$, but not $\gamma8^{-/-}$ mice, indicating that the suppression of nocifensive responding was mediated by interaction with γ8-containing AMPA receptors (Fig. 11 A). In contrast, neither the reduction in nocifensive behaviors nor the motor impairment produced by GYKI52466 were affected in γ8-deficient mice, indicating that other subtypes of AMPA receptors can support antinociceptive effects and are also responsible for motor dysfunction (Fig. 11 B, C).

Similar to intraplantar formalin, pro-inflammatory agents such as monoiodoacetic acid (MIA) or Complete Freund's Adjuvant (CFA) administered into the intra-articular space are known to increase c-fiber discharge after injection in to paw and joint (Djouhri et al., 2006; Schuelert et al., 2010). The behavioral responses to pro-inflammatory agents are characterized by shifts in weight-bearing, leading to alterations in gait. We have recently established an assay where intra-articularly administered CFA induces both spatial and temporal deficits in normal gait, revealed by forced ambulation on a treadmill which can be partially restored by a number of clinically effective drugs (i.e., opioids, NSAIDs, anti-NGF antibody) (Adams BL, 2016). A significant advantage of this assay is that it encompasses a collection of natural ambulatory endpoints (e.g., range of motion, stance/swing ratio, and paw print size) that permit a more refined examination of the effects of putative analgesics. The present studies tested the

JPET Fast Forward. Published on March 25, 2019 as DOI: 10.1124/jpet.118.250126
This article has not been copyedited and formatted. The final version may differ from this version.

hypothesis that selective blockade of γ8-containing AMPA receptors would attenuate CFA-induced gait deficits as a function of dampening glutamatergic signaling along pain pathways. Intra-articular injection of CFA rendered animals lame in the affected paw. Oral administration of LY3130481 dose-dependently restored CFA-induced gait deficits across all four indices within the composite gait score, including paw print size, stance/swing ratio, normalized stance distance and range of motion (Fig. 12, Supplemental Fig. 3 and Supplemental Video 1). The effects of LY3130481 on the composite gait score were comparable to those of Tramadol (40 mg/kg). In contrast to responses in the formalin assay, higher doses were required produce a statistically significant restoration in gait impairment.

Spinal nerve ligation (SNL) can induce a long-term sensitization of both spinal and supraspinal glutamatergic pathways that are manifest as enhanced responses to normally innocuous tactile stimuli (Kim and Chung, 1992; Leem et al., 1996; Ossipov et al., 2000). Acute spinal administration of non-selective AMPA receptor blockers has been shown to suppress the enhanced discharge of WDR spinal neurons, as well as the tactile allodynia after SNL (Leem et al., 1996). The present studies evaluated the efficacy of LY3130481 on tactile allodynia after SNL. Results showed that in contrast to gabapentin (GBP) (75 mg/kg), oral administration of LY3130481 (30 mg/kg) did not affect tactile allodynia after a single dose (Figure 12B). However, after five days of dosing, LY3130481 significantly attenuated tactile allodynia to levels equivalent to gabapentin (Figure 12B). While further studies are needed to identify the mechanism(s) responsible for the differential efficacy of LY3130481 in the repeated dosing regimen, the discrepancy may be dependent on the prolonged γ8/AMPA receptor antagonism to attenuate the sensitization of glutamatergic pathways associated with chronic nerve injury and/or an accumulation of compound and γ8/AMPA receptor occupancy at key CNS sites of action. Regardless, these data demonstrate that selective blockade of γ8-containing AMPA receptors can have beneficial effects on nocifensive behaviors in rats several weeks after nerve injury. In addition, although efficacy required multiple days of dosing, the data suggest a lack of tolerance to repeated administration of LY3130481 which is a common observation for other mechanisms of action (i.e., mu opiate receptor agonists) (Zhou et al., 2013).

4. **Discussion**

4.1 *Properties of LY3130481*

Modulation of AMPA receptors has been pursued as a therapeutic approach for numerous neurological and psychiatric disorders (O'Neill et al., 2004). Given the widespread expression of AMPA receptors, a considerable challenge has been achieving a degree of regional selectivity in altering AMPA receptor function to minimize adverse side-effects. We recently discovered LY3130481 which is a potent and selective blocker of AMPA receptors co-assembled with TARP γ8 subunits. The present studies demonstrate co-expression of γ2 with γ8 in increasing ratios reduced the potency and efficacy of LY3130481 to a much greater extent than co-expression with γ3. Consistent with these findings, the activity of LY3130481 was highest on hippocampal neurons, modestly lower on ACC and SS neurons, and significantly lower on spinal and cerebellar neurons which displayed ratios of γ8 to γ2 and/or γ3 expression of 13:1, 2:1, 0.7:1, and 0.15:1, respectively. The γ8-dependence was confirmed by the absence of activity of LY3130481 on hippocampal neurons and marked reduction on ACC neurons from γ8-deficient mice. The translatability of these findings was established by the similar potency and efficacy of LY3130481 on AMPA receptors from rodent and human cortex, spinal cord and cerebellum.. Collectively, these results indicate that the differential effects of LY3130481 are predicted by both the degree of γ8 expression, as well as the relative expression to other TARPs in distinct neuronal populations in both rodent and human brain.

4.2 *LY3130481 Modulates Glutamatergic Synaptic Transmission*

Central sensitization in spinal and supraspinal somatosensory pathways is postulated to underlie many symptoms common to chronic pain disorders (e.g., allodynia) (Latremoliere A, 2009) and depends on the initial depolarization produced by glutamate activation of AMPA receptors and sequential recruitment of NMDA receptors (Davies SN, 1987; Yoshimura M, 1990; Woolf CJ, 1991; Farkas and Ono, 1995) in response to injury of of peripheral afferents (Wall and Woolf, 1984; McNamara et al.,

2007). A critical role for γ8 TARPs in trafficking AMPA receptors to synapses, mediating excitatory transmission and underlying long-term synaptic plasticity has been established in hippocampal circuits (Rouach et al., 2005; Fukaya et al., 2006). Immunohistochemical studies have shown regional expression of γ8 in dorsal horn of the spinal cord, SS and ACC cortices and subcellular co-expression with some, but not all AMPA receptors at spinal and cortical synapses (Inamura et al., 2006; Larsson M, 2013; Sullivan SJ, 2017). These data suggested that LY3130481 should suppress, but not eliminate excitatory synaptic transmission in dorsal horn and cortical neurons. As predicted, LY3130481 attenuated AMPA receptor-dependent EPSPs, whereas GYKI53784 eliminated excitatory responses in both neuronal subtypes. Consistent with the higher total and relative (to γ2 and γ3) expression of γ8 in cortex, LY3130481 was correspondingly more potent in reducing ACC versus spinal EPSPs.

The effects of LY3130481 also were studied on the wind-up of spinal WDR neurons which depends on the interplay between AMPA and NMDA receptors (Davies SN, 1987; Yoshimura M, 1990; Stanfa and Dickenson, 1999). LY3130481 dose-dependently suppressed wind-up with a maximal efficacy of approximately 55%. LY3130481 also partially blocked responses to the initial stimulus in the train in vivo, consistent with effects on EPSPs in spinal neurons in vitro. Plasma exposures indicated that the γ8-AMPA receptor occupancy achieved with the highest dose (10 mg/kg) approached 100%, suggesting that the partial reduction in wind-up was not due to incomplete γ8-AMPA receptor occupancy, but rather to the presence of synaptic AMPA receptors devoid of γ8. Consistent with this interpretation, administration of GYKI52466 at a maximally tolerated dose (6 mg/kg, i.v.) produced a significantly greater decrease in wind-up compared to LY3130481. Interestingly, this high dose of GYKI52466 did not eliminate spinal neuron responses as observed in vitro; a similar residual response has been reported for WDR neurons after administration of the non-selective AMPA receptor blockers, NBQX or CNQX (Dougherty et al., 1992), suggesting either incomplete occupancy of AMPA receptors and/or activation of other receptor subtypes (e.g., kainate) in vivo.

JPET Fast Forward. Published on March 25, 2019 as DOI: 10.1124/jpet.118.250126
This article has not been copyedited and formatted. The final version may differ from this version.

Although the present in vivo studies focused on LY3130481 modulation of glutamaterigic signaling in spinal cord, previous studies have demonstrated a role for potentiation in the ACC in pain conditions (Bliss et al., 2016). Indeed, mechanical allodynia produced by peripheral nerve injury has been linked to AMPA receptor-dependent synaptic potentiation in ACC, whereas suppression of injury-induced potentiation is associated with an attenuation of allodynia (Li et al., 2010). These findings suggest that effects of LY3130481 on glutamate signaling and behavioral function after injury may be conferred at both spinal and supraspinal nociceptive regions of the CNS expressing γ8-containing AMPA receptors.

4.3 *LY3130481 Modulates Behavioral Responses to Injury*

The hypothesis for LY3130481 to have a wider therapeutic window in chronic pain rests on its molecular selectivity combined with the localized distribution of γ8 subunits in CNS and their fractional expression in synaptic AMPA receptors in pain pathways. The present studies demonstrate that LY3130481 partially reduces nociceptive signaling in CNS and attenuates nocifensive behaviors in rodents following formalin-induced tissue injury which increases c-fiber discharge and spinal WDR neuron activity. The magnitude of the behavioral effects were positively correlated with occupancy of γ8-AMPA receptors in CNS and abrogated in $\gamma8^{-/-}$ mice, confirming the γ8-dependence of the antinociceptive action. As importantly, the effects of LY3130481 were evident in the absence of CNS side effects (Kato et al., 2016). By contrast, the suppressive effects of GYKI52466 on formalin-induced behaviors were associated with ataxia and sedation and neither the antinociceptive nor side effects were eliminated in $\gamma8^{-/-}$ mice. These results indicate that blockade of γ8-containing AMPA receptors or other AMPA receptors can reduce nocifensive behaviors, but that the gross CNS side effects are likely dependent on AMPA receptors not assembled with γ8.

TARP γ2 subunits are expressed in dorsal horn (Larsson M, 2013; Sullivan SJ, 2017) and appear to be critical for translocation of calcium-permeable AMPA receptors at c-fiber synapses after CFA-induced peripheral inflammation (Sullivan SJ, 2017), suggesting an alternative substrate for the GYKI52466 antinociception in $\gamma8^{-/-}$ mice. Although the behavioral consequences of these γ2-dependent

JPET Fast Forward. Published on March 25, 2019 as DOI: 10.1124/jpet.118.250126
This article has not been copyedited and formatted. The final version may differ from this version.

changes have not been explored, GYKI52466 can suppress CFA-induced behaviors, possibly through blockade of γ2-containing AMPA receptors (Park JS, 2008). However, blockade of γ2-containing AMPA receptors would be expected to have concomitant motor impairment due to the high levels of expression of γ2 subunits in cerebellum (Tomita et al., 2003); an hypothesis supported by the severe motor abnormalities associated with γ2 deletion (Chen et al., 2000). Collectively, these data predict that blockade of multiple subtypes of AMPA receptor complexes may confer analgesia, and the motor impairment may be dependent on γ2-containing AMPA receptors.

The present studies also showed that LY3130481 markedly improved the composite gait score in rats after joint injury induced CFA. Examination of video recordings clearly shows that joint injury rendered animals lame and that use of the affected hindpaw during ambulation was rescued by LY3130481 treatment. Similar results have been described for clinically efficacious compounds (e.g., anti-NGF antibody) in chronic pain disorders, including those involving joint damage (Lane et al., 2010). Additional studies showed that LY3130481 was effective in reversing tactile allodynia produced by spinal nerve ligation after five, but not one day of dosing. These latter findings demonstrate the ability of γ8-AMPA antagonism to rescue a behavioral deficit after an injury has been established for multiple weeks. In addition, the data suggest that such efficacy may require sustained γ8-AMPA receptor blockade to modify the longer-lasting plasticity mechanisms in glutamatergic nociceptive pathways that have been previously described (Latremoliere A, 2009).

Given the high expression in hippocampus, an obvious concern of blocking γ8-containing AMPA receptors is disturbances in cognitive function. Recent preclinical studies have specifically addressed this possibility by testing LY3130481 in several orthogonal measures of cognitive function (Witkin et al., 2017a). Results from behavioral experiments were equivocal such that LY3130481 produced impairment in some, but not all assays and topiramate, which impacts cognitive function in humans (Wandschneider, 2017), was without effect in tests in which LY3130481 was impairing (Witkin et al., 2017a). Similarly, the γ8-dependent antagonist, JNJ-55511118, was recently reported to produce only

minor impairments in performance in the Morris water maze, the V-maze, and in a delayed non-matching to position task (Maher et al., 2016). In addition, EEG recordings showed that LY3130481 did not have sedative effects, but rather increased wake times and attenuated impairing effects of antiepileptic drugs. As well, LY3130481 increased efflux of histamine and acetylcholine in prefrontal cortex which have been associated with pro-cognitive effects in animals (Witkin et al., 2017a). While these data do not refute the possibility that LY3130481 may impact cognitive function, they underscore the need to definitively determine the relationship between any analgesic signal and cognitive impairment in the clinic.

4.4 *Anticonvulsants and Analgesics*

Anticonvulsant drugs have been used since the 1960s in pain management (Rockliff and Davis, 1966; McQuay, 1995). These drugs can have one or more mechanism of action (Bialer, 2012), including modulation of GABAergic and glutamatergic neurotransmission and/or alteration of sodium, calcium or potassium ion channels (Rogawski and Loscher, 2004), each of which has the ability to dampen the aberrant hyperexcitability of neuronal circuits associated with seizures (Bialer, 2012). We recently have demonstrated that LY3130481 can suppress seizure activity in hippocampal circuits and have marked anticonvulsant effects in multiple preclinical models of seizure (Kato et al., 2016; Witkin et al., 2017b) A similar hyperexcitability in pain pathways has been described following nerve injury and is characterized by spontaneous ectopic discharge in peripheral nerves that contributes to enhanced synaptic transmission and repetitive firing of CNS neurons, which is perceived as chronic pain (Rogawski and Loscher, 2004; Bialer, 2012). The ability of LY3130481 to dampen hyperexcitable neural circuits in tissues relevant to both seizure initiation and pain signaling is consistent with clinically efficacious molecules having both analgesic and anticonvulsant properties (e.g., carbamazepine, gabapentin). Taken together, these data prompt the hypothesis that selectively targeting γ8-containing AMPA receptors may have therapeutic potential in both seizure disorders and chronic pain conditions.

JPET Fast Forward. Published on March 25, 2019 as DOI: 10.1124/jpet.118.250126
This article has not been copyedited and formatted. The final version may differ from this version.

Acknowledgments

On 26 September 2016, Cerecor Inc. announced the acquisition of LY3130481 (now CERC-611) from Eli Lilly & Co. for development in patients with epilepsy. In addition, a patent WO 2015183673 A1 has been issued to Eli Lilly & Company for the molecule. The authors would like to thank Caryn O'Brien for technical assistance with the autoradiography experiments.

Authorship contributions

Participated in research design: Knopp, Nisenbaum, Need, Sher, Bredt, Felder, Burris, Barth, Reel, Ornstein, Gardinier, Simmons, Guo, Adams, Choong, Wall, Zwart, Schober, Kato, Porter and Swanson

Conducted experiments: Simmons, Guo, Adams, Choong, Wall, Zwart, Schober, Kato, Ding, Witkin, Porter and Swanson

Contributed new reagents or analytic tools: Barth, Reel, Ornstein, Gardinier, Ding, Witkin, Gernert, Wang, Qian and Porter

Performed data analysis: Knopp, Nisenbaum, Need, Sher, Burris, Simmons, Guo, Adams, Choong, Wall, Zwart, Schober, Kato and Catlow

Wrote or contributed to the writing of the manuscript: Knopp, Nisenbaum, Need, Sher, Bredt, Felder, Simmons, Guo, Adams, Choong, Wall, Zwart, Schober and Kato

References

Abbott FV FK, Westbrook RF (1995) The formalin test: scoring properties of the first and second phases of the pain response in rats. *Pain* **60**:91-102.

Adams BL GW, Gors RT, Knopp KL (2016) Pharmacological interrogation of a rodent forced ambulation model: leveraging gait impairment as a measure of pain behavior pre-clinically. *Osteoarthritis & Cartilage* **24**:1928-1939.

Barth VN, Chernet E, Martin LJ, Need AB, Rash KS, Morin M and Phebus LA (2006) Comparison of rat dopamine D2 receptor occupancy for a series of antipsychotic drugs measured using radiolabeled or nonlabeled raclopride tracer. *Life Sci* **78**:3007-3012.

Baumbarger PJ, Muhlhauser M, Zhai J, Yang CR and Nisenbaum ES (2001) Positive modulation of alpha-amino-3-hydroxy-5-methyl-4-isoxazole propionic acid (AMPA) receptors in prefrontal cortical pyramidal neurons by a novel allosteric potentiator. *J Pharmacol Exp Ther* **298**:86-102.

Bee LA and Dickenson AH (2009) Effects of lacosamide, a novel sodium channel modulator, on dorsal horn neuronal responses in a rat model of neuropathy. *Neuropharmacology* **57**:472-479.

Bialer M (2012) Why are antiepileptic drugs used for nonepileptic conditions? *Epilepsia* **53 Suppl 7**:26-33.

Bliss TV, Collingridge GL, Kaang BK and Zhuo M (2016) Synaptic plasticity in the anterior cingulate cortex in acute and chronic pain. *Nat Rev Neurosci* **17**:485-496.

Chaplan SR, Bach FW, Pogrel JW, Chung JM and Yaksh TL (1994) Quantitative assessment of tactile allodynia in the rat paw. *J Neurosci Methods* **53**:55-63.

Chapman V and Dickenson AH (1995) Time-related roles of excitatory amino acid receptors during persistent noxiously evoked responses of rat dorsal horn neurones. *Brain Res* **703**:45-50.

Chen L, Chetkovich DM, Petralia RS, Sweeney NT, Kawasaki Y, Wenthold RJ, Bredt DS and Nicoll RA (2000) Stargazin regulates synaptic targeting of AMPA receptors by two distinct mechanisms. *Nature* **408**:936-943.

Chernet E, Martin LJ, Li D, Need AB, Barth VN, Rash KS and Phebus LA (2005) Use of LC/MS to assess brain tracer distribution in preclinical, in vivo receptor occupancy studies: dopamine D2, serotonin 2A and NK-1 receptors as examples. *Life Sci* **78**:340-346.

Coderre TJ FM, McKenna JE, Dalal S, Melzack R (1993) The formalin test: a validation of the weighted-scores method of behavioural pain rating. *Pain* **54**:43-50.

Coderre TJ and Melzack R (1992) The contribution of excitatory amino acids to central sensitization and persistent nociception after formalin-induced tissue injury. *J Neurosci* **12**:3665-3670.

Davies SN LD (1987) Evidence for involvement of N-methylaspartate receptors in 'wind-up' of class 2 neurones in the dorsal horn of the rat. *Brain Res* **424**:402-406.

Dickenson AH (1990) A cure for wind up: NMDA receptor antagonists as potential analgesics. *Trends Pharmacol Sci* **11**:307-309.

Dickenson AH and Sullivan AF (1987) Evidence for a role of the NMDA receptor in the frequency dependent potentiation of deep rat dorsal horn nociceptive neurones following C fibre stimulation. *Neuropharmacology* **26**:1235-1238.

Djouhri L, Koutsikou S, Fang X, McMullan S and Lawson SN (2006) Spontaneous pain, both neuropathic and inflammatory, is related to frequency of spontaneous firing in intact C-fiber nociceptors. *J Neurosci* **26**:1281-1292.

Dougherty PM, Palecek J, Paleckova V, Sorkin LS and Willis WD (1992) The role of NMDA and non-NMDA excitatory amino acid receptors in the excitation of primate spinothalamic tract neurons by mechanical, chemical, thermal, and electrical stimuli. *J Neurosci* **12**:3025-3041.

Eusebi F, Palma E, Amici M and Miledi R (2009) Microtransplantation of ligand-gated receptor-channels from fresh or frozen nervous tissue into Xenopus oocytes: a potent tool for expanding functional information. *Prog Neurobiol* **88**:32-40.

Farkas S and Ono H (1995) Participation of NMDA and non-NMDA excitatory amino acid receptors in the mediation of spinal reflex potentials in rats: an in vivo study. *Br J Pharmacol* **114**:1193-1205.

Fukaya M, Tsujita M, Yamazaki M, Kushiya E, Abe K, Natsume R, Kano M, Kamiya H, Watanabe M and Sakimura K (2006) Abundant distribution of TARP gamma-8 in synaptic and extrasynaptic surface of hippocampal neurons and its major role in AMPA receptor expression on spines and dendrites. *Eur J Neurosci* **24**:2177-2190.

Gardinier KM, Gernert DL, Porter WJ, Reel JK, Ornstein PL, Spinazze P, Stevens FC, Hahn P, Hollinshead SP, Mayhugh D, Schkeryantz J, Khilevich A, De Frutos O, Gleason SD, Kato AS, Luffer-Atlas D, Desai PV, Swanson S, Burris KD, Ding C, Heinz BA, Need AB, Barth VN, Stephenson GA, Diseroad BA, Woods TA, Yu H, Bredt D and Witkin JM (2016) The Discovery of The First alpha-Amino-3-Hydroxy-5-Methyl-4-Isoxazolepropionic Acid (AMPA) Receptor Antagonist Dependent Upon Transmembrane AMPA Receptor Regulatory Protein (TARP) Gamma-8. *J Med Chem* **59**:4753-4768.

Gill MB, Kato AS, Roberts MF, Yu H, Wang H, Tomita S and Bredt DS (2011) Cornichon-2 modulates AMPA receptor-transmembrane AMPA receptor regulatory protein assembly to dictate gating and pharmacology. *J Neurosci* **31**:6928-6938.

Gill MB, Kato AS, Wang H and Bredt DS (2012) AMPA receptor modulation by cornichon-2 dictated by transmembrane AMPA receptor regulatory protein isoform. *Eur J Neurosci* **35**:182-194.

Haley J, Ketchum S and Dickenson A (1990) Peripheral kappa-opioid modulation of the formalin response: an electrophysiological study in the rat. *Eur J Pharmacol* **191**:437-446.

Herrero JF, Laird JM and Lopez-Garcia JA (2000) Wind-up of spinal cord neurones and pain sensation: much ado about something? *Prog Neurobiol* **61**:169-203.

Hunter JC SL (1994) Role of Excitatory Amino Acid Receptors in the Mediation of the Nociceptive Response to Formalin in the Rat. *Neurosci Lett* **174**:217-221.

Inamura M, Itakura M, Okamoto H, Hoka S, Mizoguchi A, Fukazawa Y, Shigemoto R, Yamamori S and Takahashi M (2006) Differential localization and regulation of stargazin-like protein, gamma-8 and stargazin in the plasma membrane of hippocampal and cortical neurons. *Neurosci Res* **55**:45-53.

Jackson AC and Nicoll RA (2011) The expanding social network of ionotropic glutamate receptors: TARPs and other transmembrane auxiliary subunits. *Neuron* **70**:178-199.

Kato AS, Burris KD, Gardinier KM, Gernert DL, Porter WJ, Reel J, Ding C, Tu Y, Schober DA, Lee MR, Heinz BA, Fitch TE, Gleason SD, Catlow JT, Yu H, Fitzjohn SM, Pasqui F, Wang H, Qian Y, Sher E, Zwart R, Wafford KA, Rasmussen K, Ornstein PL, Isaac JT, Nisenbaum ES, Bredt DS and Witkin JM (2016) Forebrain-selective AMPA-receptor antagonism guided by TARP gamma-8 as an antiepileptic mechanism. *Nat Med* **22**:1496-1501.

Kato AS, Gill MB, Ho MT, Yu H, Tu Y, Siuda ER, Wang H, Qian YW, Nisenbaum ES, Tomita S and Bredt DS (2010) Hippocampal AMPA Receptor Gating Controlled by Both TARP and Cornichon Proteins. *Neuron* **68**:1082-1096.

Kato AS and Witkin JM (2018) Auxiliary subunits of AMPA receptors: the discovery of a forebrain-selective antagonist, LY3130481/CERC-611. *Biochem Pharmacol* **147**:191-200.

Kim SH and Chung JM (1992) An experimental model for peripheral neuropathy produced by segmental spinal nerve ligation in the rat. *Pain* **50**:355-363.

Lane NE, Schnitzer TJ, Birbara CA, Mokhtarani M, Shelton DL, Smith MD and Brown MT (2010) Tanezumab for the treatment of pain from osteoarthritis of the knee. *N Engl J Med* **363**:1521-1531.

Larsson M AN, Watanabe M, Svensson CI (2013) Distribution of transmembrane AMPA receptor regulatory protein (TARP) isoforms in the rat spinal cord. *Neuroscience* **248**:180-193.

Latremoliere A WC (2009) Central sensitization: a generator of pain hypersensitivity by central neural plasticity. *Journal of Pain* **10**:895-926.

Lee MR, Gardinier KM, Gernert DL, Schober DA, Wright RA, Wang H, Qian Y, Witkin JM, Nisenbaum ES and Kato AS (2017) Structural Determinants of the gamma-8 TARP Dependent AMPA Receptor Antagonist. *ACS Chem Neurosci* **8**:2631-2647.

Leem JW, Choi EJ, Park ES and Paik KS (1996) N-methyl-D-aspartate (NMDA) and non-NMDA glutamate receptor antagonists differentially suppress dorsal horn neuron responses to mechanical stimuli in rats with peripheral nerve injury. *Neurosci Lett* **211**:37-40.

Lein ES, Hawrylycz MJ, Ao N, Ayres M, Bensinger A, Bernard A, Boe AF, Boguski MS, Brockway KS, Byrnes EJ, Chen L, Chen L, Chen TM, Chin MC, Chong J, Crook BE, Czaplinska A, Dang CN, Datta S, Dee NR, Desaki AL, Desta T, Diep E, Dolbeare TA, Donelan MJ, Dong HW, Dougherty JG, Duncan BJ, Ebbert AJ, Eichele G, Estin LK, Faber C, Facer BA, Fields R, Fischer SR, Fliss TP, Frensley C, Gates SN, Glattfelder KJ, Halverson KR, Hart MR, Hohmann JG, Howell MP, Jeung DP, Johnson RA, Karr PT, Kawal R, Kidney JM, Knapik RH, Kuan CL, Lake JH, Laramee AR, Larsen KD, Lau C, Lemon TA, Liang AJ, Liu Y, Luong LT, Michaels J, Morgan JJ, Morgan RJ, Mortrud MT, Mosqueda NF, Ng LL, Ng R, Orta GJ, Overly CC, Pak TH, Parry SE, Pathak SD, Pearson OC, Puchalski RB, Riley ZL, Rockett HR, Rowland SA, Royall JJ, Ruiz MJ, Sarno NR, Schaffnit K, Shapovalova NV, Sivisay T, Slaughterbeck CR, Smith SC, Smith KA, Smith BI, Sodt AJ, Stewart NN, Stumpf KR, Sunkin SM, Sutram M, Tam A, Teemer CD, Thaller C, Thompson CL, Varnam LR, Visel A, Whitlock RM, Wohnoutka PE, Wolkey CK, Wong VY, et al. (2007) Genome-wide atlas of gene expression in the adult mouse brain. *Nature* **445**:168-176.

Li XY, Ko HG, Chen T, Descalzi G, Koga K, Wang H, Kim SS, Shang Y, Kwak C, Park SW, Shim J, Lee K, Collingridge GL, Kaang BK and Zhuo M (2010) Alleviating neuropathic pain hypersensitivity by inhibiting PKMzeta in the anterior cingulate cortex. *Science* **330**:1400-1404.

Maher MP, Wu N, Ravula S, Ameriks MK, Savall BM, Liu C, Lord B, Wyatt RM, Matta JA, Dugovic C, Yun S, Ver Donck L, Steckler T, Wickenden AD, Carruthers NI and Lovenberg TW (2016) Discovery and Characterization of AMPA Receptor Modulators Selective for TARP-gamma8. *J Pharmacol Exp Ther* **357**:394-414.

McCall WD, Tanner KD and Levine JD (1996) Formalin induces biphasic activity in C-fibers in the rat. *Neurosci Lett* **208**:45-48.

McNamara CR, Mandel-Brehm J, Bautista DM, Siemens J, Deranian KL, Zhao M, Hayward NJ, Chong JA, Julius D, Moran MM and Fanger CM (2007) TRPA1 mediates formalin-induced pain. *Proc Natl Acad Sci U S A* **104**:13525-13530.

McQuay HJ (1995) Pre-emptive analgesia: a systematic review of clinical studies. *Ann Med* **27**:249-256.

Menuz K, Kerchner GA, O'Brien JL and Nicoll RA (2009) Critical role for TARPs in early development despite broad functional redundancy. *Neuropharmacology* **56**:22-29.

Miledi R, Eusebi F, Martinez-Torres A, Palma E and Trettel F (2002) Expression of functional neurotransmitter receptors in Xenopus oocytes after injection of human brain membranes. *Proc Natl Acad Sci U S A* **99**:13238-13242.

Miledi R, Palma E and Eusebi F (2006) Microtransplantation of neurotransmitter receptors from cells to Xenopus oocyte membranes: new procedure for ion channel studies. *Methods Mol Biol* **322**:347-355.

Monyer H, Seeburg PH and Wisden W (1991) Glutamate-operated channels: developmentally early and mature forms arise by alternative splicing. *Neuron* **6**:799-810.

Nishiyama T GL, Lee C, Kawasaki-Yatsugi S, Yamaguchi T (1999) The Systemically Administered Competitive AMPA Receptor Antagonist, YM872, has Analgesic Effects on Thermal or Formalin-induced Pain in Rats. *Anesthesia & Analgesia* **89**:1534-1537.

O'Neill MJ, Murray TK, Whalley K, Ward MA, Hicks CA, Woodhouse S, Osborne DJ and Skolnick P (2004) Neurotrophic actions of the novel AMPA receptor potentiator, LY404187, in rodent models of Parkinson's disease. *Eur J Pharmacol* **486**:163-174.

Olsen RW SO, Houser CR (1987) [3H]AMPA Binding to Glutamate Receptor Subpopulations in Rat Brain. *Brain Res* **402**:243-254.

Ossipov MH, Lai J, Malan TP, Jr. and Porreca F (2000) Spinal and supraspinal mechanisms of neuropathic pain. *Ann N Y Acad Sci* **909**:12-24.

Park JS YM, Guan X, Xu JT, Shih MH, Guan Y, Raja SN, Tao YX (2008) Role of spinal cord alpha-amino-3-hydroxy-5-methyl-4-isoxazolepropionic acid receptors in complete Freund's adjuvant-induced inflammatory pain. *Molecular Pain* **4**:67.

Rockliff BW and Davis EH (1966) Controlled sequential trials of carbamazepine in trigeminal neuralgia. *Archives of neurology* **15**:129-136.

Rogawski MA and Loscher W (2004) The neurobiology of antiepileptic drugs for the treatment of nonepileptic conditions. *Nat Med* **10**:685-692.

Rouach N, Byrd K, Petralia RS, Elias GM, Adesnik H, Tomita S, Karimzadegan S, Kealey C, Bredt DS and Nicoll RA (2005) TARP gamma-8 controls hippocampal AMPA receptor number, distribution and synaptic plasticity. *Nat Neurosci* **8**:1525-1533.

Schuelert N, Zhang C, Mogg AJ, Broad LM, Hepburn DL, Nisenbaum ES, Johnson MP and McDougall JJ (2010) Paradoxical effects of the cannabinoid CB2 receptor agonist GW405833 on rat osteoarthritic knee joint pain. *Osteoarthritis Cartilage* **18**:1536-1543.

Schwenk J, Harmel N, Brechet A, Zolles G, Berkefeld H, Muller CS, Bildl W, Baehrens D, Huber B, Kulik A, Klocker N, Schulte U and Fakler B (2012) High-resolution proteomics unravel architecture and molecular diversity of native AMPA receptor complexes. *Neuron* **74**:621-633.

Schwenk J, Harmel N, Zolles G, Bildl W, Kulik A, Heimrich B, Chisaka O, Jonas P, Schulte U, Fakler B and Klocker N (2009) Functional proteomics identify cornichon proteins as auxiliary subunits of AMPA receptors. *Science* **323**:1313-1319.

Simmons RM, Forster B, Guo W and Knopp KL (2014) A method to enhance the magnitude of tactile hypersensitivity following spinal nerve ligation in rats. *J Neurosci Methods* **233**:50-53.

Simmons RM LD, Hoo KH, Ornstein PL, Iyengar S (1998) Kainate GluR5 receptor subtype mediates the nociceptive response to formalin in the rat. *Neuropharmacology* **37**:25-36.

Sommer B, Keinanen K, Verdoorn TA, Wisden W, Burnashev N, Herb A, Kohler M, Takagi T, Sakmann B and Seeburg PH (1990) Flip and flop: a cell-specific functional switch in glutamate-operated channels of the CNS. *Science* **249**:1580-1585.

Stanfa LC and Dickenson AH (1999) The role of non-N-methyl-D-aspartate ionotropic glutamate receptors in the spinal transmission of nociception in normal animals and animals with carrageenan inflammation. *Neuroscience* **93**:1391-1398.

Sullivan SJ FM, Cull-Candy SG (2017) TARP γ-2 Is Required for Inflammation-Associated AMPA Receptor Plasticity within Lamina II of the Spinal Cord Dorsal Horn. *Journal of Neuroscience* **37**:6007-6020.

Svendsen F, Tjolsen A and Hole K (1998) AMPA and NMDA receptor-dependent spinal LTP after nociceptive tetanic stimulation. *Neuroreport* **9**:1185-1190.

Tomita S, Chen L, Kawasaki Y, Petralia RS, Wenthold RJ, Nicoll RA and Bredt DS (2003) Functional studies and distribution define a family of transmembrane AMPA receptor regulatory proteins. *J Cell Biol* **161**:805-816.

Wall PD and Woolf CJ (1984) Muscle but not cutaneous C-afferent input produces prolonged increases in the excitability of the flexion reflex in the rat. *J Physiol* **356**:443-458.

Wandschneider B, Burdett, J., Townsend, L., Hill, A., Thompson, P.J, Duncan, J.S., Koepp, M.J. (2017) Effect of Topiramate and Zonisamide on fMRI Cognitive Networks. *Neurology* **88**:1165-1171.

Wheeler-Aceto H PF, Cowan A (1990) The rat paw formalin test: comparison of noxious agents. *Pain* **40**:229-238.

Witkin JM, Li J, Gilmour G, Mitchell SN, Carter G, Gleason SD, Seidel WF, Eastwood BJ, McCarthy A, Porter WJ, Reel J, Gardinier KM, Kato AS and Wafford KA (2017a) Electroencephalographic, cognitive, and neurochemical effects of LY3130481 (CERC-611), a selective antagonist of TARP-gamma8-associated AMPA receptors. *Neuropharmacology* **126**:257-270.

Witkin JM, Schober DA, Gleason SD, Catlow JT, Porter WJ, Reel J, Jin X, Hobbs J, Gehlert D, Gernert DL, Gardinier KM, Kato AS, Ping X and Smith JL (2017b) Targeted Blockade of TARP-g8-Associated AMPA Receptors: Anticonvulsant Activity with the Selective Antagonist LY3130481 (CERC-611). *CNS Neurol Disord Drug Targets* **16**:1099-1110.

Woolf CJ TS (1991) The induction and maintenance of central sensitization is dependent on N-methyl-D-aspartic acid receptor activation; implications for the treatment of post-injury pain hypersensitivity states. *Pain* **44**:293-299.

Yoshimura M JT (1990) Amino acid-mediated EPSPs at primary afferent synapses with substantia gelatinosa neurones in the rat spinal cord. *Journal of Physiology* **430**:315-335.

Zhou Q, Wang J, Zhang X, Zeng L, Wang L and Jiang W (2013) Effect of metabotropic glutamate 5 receptor antagonists on morphine efficacy and tolerance in rats with neuropathic pain. *Eur J Pharmacol* **718**:17-23.

Footnote

* Dr. Knopp reports financial support (salaries) for all authors from Eli Lilly & Company, outside the submitted work.

JPET Fast Forward. Published on March 25, 2019 as DOI: 10.1124/jpet.118.250126
This article has not been copyedited and formatted. The final version may differ from this version.

Legends for Figures

Figure 1. The potency and efficacy of LY3130481 is determined by the amounts of γ2 or γ3 co-transfected with γ8 (A) Representative current traces recorded from HEK293T cells recombinantly expressing GluA1i alone, in combination with γ2, γ3 or γ8 alone or with different amounts of γ8 and γ2 or γ3. Note that the initial inward currents in Figure 1 and subsequent figures do not reflect the peak of the glutamate-evoked current due to the slower perfusion system used in these experiments. LY3130481 potently blocked currents from GluA1i/γ8 receptors, but had minimal to no effect of GluA1i receptors alone or in combination with γ2 or γ3. Note the unique resensitization property of glutamate-evoked currents in GluA1/γ8 receptors (arrow). Co-transfection of GluA1i with γ8 and different ratios of γ2 or γ3 reduced the potency and efficacy of LY3130481 on Glu-evoked currents compared to GluA1/γ8 receptors alone. Note the elimination of resensitization in receptors co-expressed with γ8 and γ2 or γ3 subunits. **(B,C)** Concentration-response profiles of LY3130481 on recombinant GluA1 receptors co-transfected with γ2, γ3 and γ8 in different ratios. The relative amplitudes of glutamate-evoked steady-state currents are plotted as a function of LY3130481 concentration. Co-transfection of γ2 with γ8 in increasing ratios had a profound effect on the potency and efficacy of LY3130481. In contrast, co-transfection of γ3 with γ8 had more modest effects on the activity of LY3130481. The relative $I_{Glu\ Steady\text{-}state}$ was calculated by dividing the current amplitude at the end of the glutamate application before and after exposure to LY3130481. Symbols reflect means ± SEM, *n*=3-6 recordings/concentration. The IC_{50} and Imax values for each transfectant are presented in Supplemental Table 1.

Figure 2. The potency and efficacy of GYKI52466 is independent of TARP subunit expression (A) Representative current traces recorded from HEK293T cells recombinantly expressing GluA1i in combination with γ2 or γ8 alone or with after co-tranfection of γ2 and γ8 in a ratio of 10:1. GYKI52466 blocked currents from GluA1i/γ8 (*n*=4) GluA1i/γ2 (*n*=5) receptors with similar potency. Co-transfection of GluA1i with γ2 and γ8 in a ratio of 10:1 did not affect the potency of GYKI52466 on Glu-evoked

currents compared to GluA1/γ8 receptors alone. Note the elimination of resensitization in receptors co-expressed with γ8 and γ2 subunits. **(B)** Concentration-response profiles of GYKI52466 on recombinant GluA1i receptors co-transfected with γ2 and γ8 in different ratios. The relative amplitudes of glutamate-evoked steady-state currents are plotted as a function of GYKI52466 concentration. Co-transfection of γ2 with γ8 in increasing ratios (*n*=5) had no effect on the potency and efficacy of GYKI52466. **(C)** Concentration-response profiles of GYKI52466 on acutely isolated hippocampal pyramidal neurons (*n*=6), ACC pyramidal neurons (*n*=5), and cerebellar Purkinje neurons (*n*=4). GYKI52466 did not differentially affect glutamate-evoked currents from these cell types. The relative $I_{Glu\ Steady\text{-}state}$ was calculated by dividing the current amplitude at the end of the glutamate application before and after exposure to GYKI52466. Symbols reflect means ± SEM. The IC_{50} and Imax values for each transfectant are presented in Supplemental Table 2.

Figure 3. Expression of TARP subunits in tissue from rat brain and spinal cord. (A-D) qPCR methods measured expression of γ2, γ3, and γ8 in hippocampus, frontal cortex, cerebellum and the lumbar region of spinal cord. Consistent with previous reports, γ8 expression was highest in hippocampus followed by frontal cortex, spinal cord and cerebellum. Highest expression of γ2 subunit was in cerebellum and γ3 was in frontal cortex. The relative expression levels of γ2 and γ3 were significantly lower than γ8 in hippocampus and frontal cortex. The relative expression of γ2 and γ8 was similar in spinal cord and significantly different from γ3 and the expression level of γ2 was higher than γ3 or γ8 in cerebellum Data presented in graphs are relative expression to Hprt1, expressed as ΔΔCt (ΔΔCt= ΔCtgene- ΔCtnormalizer (Hprt1)). Statistical analyses conducted using one-way ANOVA followed by Dunnet's post-hoc test, ***= p<.0001, *n*=5 for each group. Receptor density in spinal cord and brain slices from $\gamma8^{+/+}$ **(E,F)** and $\gamma8^{-/-}$ **(G,H)** mice using [^{3}H]-LY3074158. **(I,J)** Expression pattern of the CACNG8 mRNA by in situ hybridization in a coronal section of mouse spinal cord and sagittal section of mouse brain from the Allen Mouse Brain Atlas (Lein et al., 2007). **(K)** Total binding densities measured in hippocampus (*n*=8), spinal cord (*n*=12) and cerebellum (*n*=8) from $\gamma8^{+/+}$ and $\gamma8^{-/-}$ mice.

Statistical analyses conducted using one-way ANOVA followed by Dunnet's post-hoc test, ***= p<.0001. Hipp = hippocampus, SC = spinal cord, Cblm = cerebellum.

Figure 4. Differential effects of LY3130481 on native AMPA receptors from neurons acutely isolated from rat brain and spinal cord. (A) Concentration-response profiles of LY3130481 on several neuronal cell types. The relative amplitudes of glutamate-evoked steady-state currents are plotted as a function of LY3130481 concentration. LY3130481 potently and efficaciously blocked responses from hippocampal and cortical (ACC and SS) neurons, but not from cerebellar Purkinje neurons. The AMPA receptor-mediated responses from spinal neurons were also blocked by LY3130481, albeit at higher concentrations. Symbols represent means ± SEM.

(B) Concentration-response profiles of LY3130481 on glutamate-evoked currents recorded from acutely-isolated hippocampal and ACC neurons from $\gamma8^{+/+}$ or $\gamma8^{-/-}$ mice. Relative amplitudes of glutamate-evoked steady-state currents are plotted as a function of LY3130481 concentration. LY3130481 potently and efficaciously blocked responses from hippocampal and ACC neurons; effects that were eliminated or markedly reduced in neurons from $\gamma8^{-/-}$ mice. Symbols represent means ± SEM.

Figure 5. Differential effects of LY3130481 on native AMPA receptors from human brain and spinal cord. (A,C,E) Representative current traces evoked by application of AMPA + cyclothiazide (CTZ) on Xenopus oocytes micro-implanted with human, cortical, spinal cord or cerebellar tissue. LY3130481 (10 μM) was co-applied after application of AMPA (100 μM) + CTZ (30 μM). Note that LY3130481 produced a near-complete suppression of cortical AMPA receptors responses, a partial block of spinal cord AMPA receptor activity, and minimal effect on cerebellar AMPA receptors responses. **(B,D)** The amplitude of AMPA + CTZ-evoked currents in the absence and presence of LY3130481 were measured at the time points indicated by the arrows in A and C. The current amplitudes in the presence of LY3130481 were normalized to the pre-drug amplitude and plotted as a function of LY3130481 concentration for cortical **(B)** and spinal cord **(D)** AMPA receptors. Symbols reflect means ± SEM, *n*=2-5 recordings/concentration.

JPET Fast Forward. Published on March 25, 2019 as DOI: 10.1124/jpet.118.250126
This article has not been copyedited and formatted. The final version may differ from this version.

Figure 6. LY3130481 suppresses AMPA receptor-dependent EPSPs in rat ACC pyramidal neurons and dorsal horn spinal cord neurons *in vitro*. (A) Plot of EPSP amplitudes in ACC neurons in control solution (*n*=4) or in the presence of LY3130481 (0.3, 3.0 μM) (*n*=4) as a function of time from recording onset. **(B)** Plot of the normalized EPSP amplitude (mean ± SEM) in ACC neurons in control solution (*n*=4) or solutions containing LY3130481 (0.3, 3.0 μM) (*n*=4) or GYKI53784 (50 μM) (*n*=4). **(C)** Plot of EPSP amplitudes in spinal neurons in control solution (*n*=4) or in the presence of LY3130481 (0.3, 3.0 μM) (*n*=4) as a function of time from recording onset. **(D)** Plot of the normalized EPSP amplitude in spinal neurons in control solution (*n*=4) or solutions containing LY3130481 (0.3, 3.0 μM) (*n*=4) or GYKI (50 μM) (*n*=4).*** p<.001, **** p<0.0001.

Figure 7. Pharmacokinetics and receptor occupancy for LY3130481 in rat. (A) Plot of plasma concentration of LY3130481 as a function of time in Sprague-Dawley rats following intravenous (1 mg/kg) or oral (3 mg/kg) administration. **(B)** The percent receptor occupancy of γ8-containing AMPA receptors for each dose of LY3130481 (0.1-3.0 mg/kg, p.o.) is plotted as a function plasma concentrations. In these experiments, 30 mg/kg of LY3130481 was associated with occupancy levels approaching 100%. Symbols represent means ± SEMs.

Figure 8. LY3130481 attenuates wind-up discharge of spinal sensory neurons. (A) Extracellular single unit recordings from WDR neurons in the dorsal horn of the lumbar spinal cord region *in vivo* in response to repetitive stimulation of the receptive field in the hindpaw. A train of 16 stimuli delivered at 1 Hz (arrows) elicited responses from sensory neurons characterized by an increase in discharge probability in response to later stimuli in the train compared to earlier stimuli (wind-up). As well, several seconds of ongoing discharge could be observed following the last stimulus in the train (after-discharge). Intravenous administration of vehicle had minimal effect on wind-up or after-discharge. In contrast, LY3130481 (1-10 mg/kg) dose-dependently reduced the number of discharges over the course of the train of stimuli. After-discharges also were suppressed. **(B)** Plot of the wind-up response of spinal neurons (normalized to baseline responses, mean ± SEMs) following intravenous

administration of vehicle (*n*=8) and LY3130481 (1-10 mg/kg, *n*=7-8) or GYKI (6 mg/kg, *n*=4)). **(C)** Plot of the number of discharges of spinal neurons in response to the first stimulus in the 16-stimulus train (mean ± SEMs) following intravenous administration of vehicle (*n*=8) and LY3130481 (1-10 mg/kg, *n*=7-8)) or GYKI (6 mg/kg, *n*=5)). * p<.05, ** p<.01, *** p<.001.

Figure 9. LY3130481 reduces formalin-induced nocifensive behavior in rats. (A) Oral administration of LY3130481 (0.3–30 mg/kg, 30 min pretreatment) dose-dependently attenuated formalin-induced paw licking behavior in Sprague-Dawley rats. The positive control, tramadol (40 mg/kg) was also effective in decreasing paw licking. Effects of both drugs were observed on in both the early (0-5 min) and late (10-60 min) phases of the formalin-induced behavioral profile. The ED_{50} for LY3130481 was 3.7 mg/kg. Bars represent means + SEMs, *n*=8-16 animals per group. **=p<.01, ***=p>.001, ****= p<.0001. **(B)** Plot of the dose-dependence of the percent suppression of nocifensive responsding in the late phase of the formalin response (from **A**) versus the percent CNS γ8/AMPA receptor occupancy (from Fig. 7B) for LY3130481. Results show that the dose-dependent increase in CNS γ8/AMPA receptor occupancy is associated with an increase in the suppression of nocifensive behaviors after formalin treatment. Symbols represent means + SEMs, *n*=8-16 animals per group.

Figure 10. LY3130481, but not GYKI52466, reduces formalin-induced behavior in mice without motor impairment. (A,B) Oral administration of LY3130481 (1-10 mg/kg, 30 min pretreatment) or GYKI52466 (3-30 mg/kg) dose-dependently attenuated formalin-induced paw licking behavior in CD-1 mice. The positive control, Tramadol (40 mg/kg) was also effective in decreasing paw licking. Effects of all drugs were observed on in both the early (0-5 min) and late (10-60 min) phases of the formalin-induced behavioral profile. The ED_{50} for LY3130481 was 4.7 mg/kg, whereas the ED_{50} for GYKI52466 was 13.4 mg/kg. Bars represent means ± SEMs, *n*=10 animals per group. Statistical analyses conducted using two-way ANOVA followed by Dunnet's post-hoc test, ***=p<0.0001. **(C,D)** Rotorod performance was measured following oral administration of LY3130481 and GYKI across the efficacious dose range for each compound. LY3130481 did not impair rotorod performance at either

30 or 60 minutes post-dosing. Conversely, administration of GYKI52466 at 20 and 30 mg/kg produced significant impairment in motor performance as evidenced by an inability to remain on the rotorod for the entire two min testing period at 30 and 60 min post-dosing. Bars represent means ± SEMs, *n*=10 animals per group. Statistical analyses conducted using two-way ANOVA followed by Dunnet's post-hoc test, ***=p<0.0001.

Figure 11. Attenuation of mouse formalin-induced nocifensive behavior by LY3130481, but not GYKI52466 is γ8-dependent. The calculated ED_{50} values for LY3130481 (4.7 mg/kg) and GYKI52466 (13.4 mg/kg) derived from dose-response experiments in $\gamma8^{+/+}$ mice (see Figure 10) were evaluated in $\gamma8^{+/+}$ or $\gamma8^{-/-}$ mice. **(A)** LY3130481 significantly decreased formalin-induced nocifensive behavior in the late phase in $\gamma8^{+/+}$ mice, butdid not affect paw-licking in the $\gamma8^{-/-}$ mice, **(B)** Conversely, the suppressive effects of GYKI52466 on formalin-induced paw licking were evident in both $\gamma8^{+/+}$ or $\gamma8^{-/-}$ mice. **(C)** The motor impairing effects of GYKI52466 (13.4 mg/kg, p.o.) observed in $\gamma8^{+/+}$ mice were retained in $\gamma8^{-/-}$ mice. Bars represent means + SEMs, *n*=10 animals per group. *=p<0.05.

Figure 12. LY3130481 attenuates CFA-induced gait deficits and tactile allodynia after spinal nerve ligation in rats. (A) Intra-articular CFA administration produced profound gait impairment in female Sprague-Dawley rats, leading to the avoidance of weight-bearing during forced ambulation (Baseline, 2 days post-CFA). Oral administration of LY3130481 (1-30 mg/kg) dose-dependently attenuated gait deficits when administered 3 days post-CFA, as measured by the composite gait score. Tramadol (40 mg/kg, p.o.) also significantly reduced deficits in gait. Bars represent means ± SEMs, *n*=8 animals per group. * =p<0.05 vs vehicle. **(B)** Ligation of the L5 and L6 spinal nerves produces a marked decrease in the withdrawal threshold (tactile allodynia) of the injured hindpaw as measured by probing with graded von Frey filaments. Administration of gabapentin (GBP, 75 mg/kg, p.o.) reversed tactile allodynia on both Day 1 and Day 5 of dosing. In contrat, LY3130481 (30 mg/kg, p.o.) had no effect after one day of dosing, but did produce a significant reversal of tactile allodynia after five days of dosing.. Data expressed as response (grams), gram force applied to the hindpaw ipsilateral to the

ligation. Bars represent means ± SEM withdrawal thresholds. *p<0.XX, **p<0.XX ***p<0.XX, Mean S.E. , p 0.05 compared with vehicle; #, p 0.1 compared with vehicle. BL= baseline, Post-SNL= post-spinal nerve ligation.

JPET Fast Forward. Published on March 25, 2019 as DOI: 10.1124/jpet.118.250126
This article has not been copyedited and formatted. The final version may differ from this version.

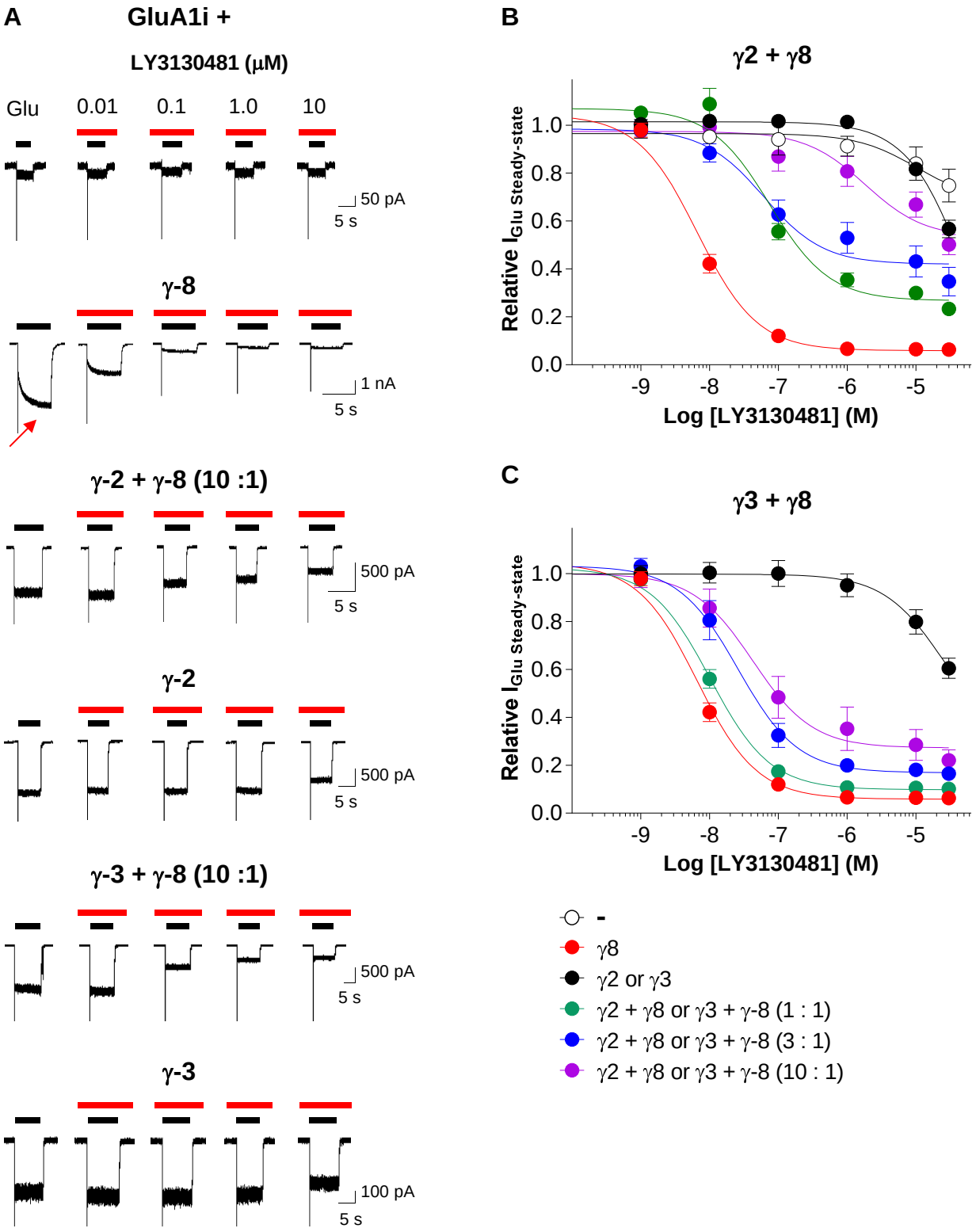

Figure 1

JPET Fast Forward. Published on March 25, 2019 as DOI: 10.1124/jpet.118.250126
This article has not been copyedited and formatted. The final version may differ from this version.

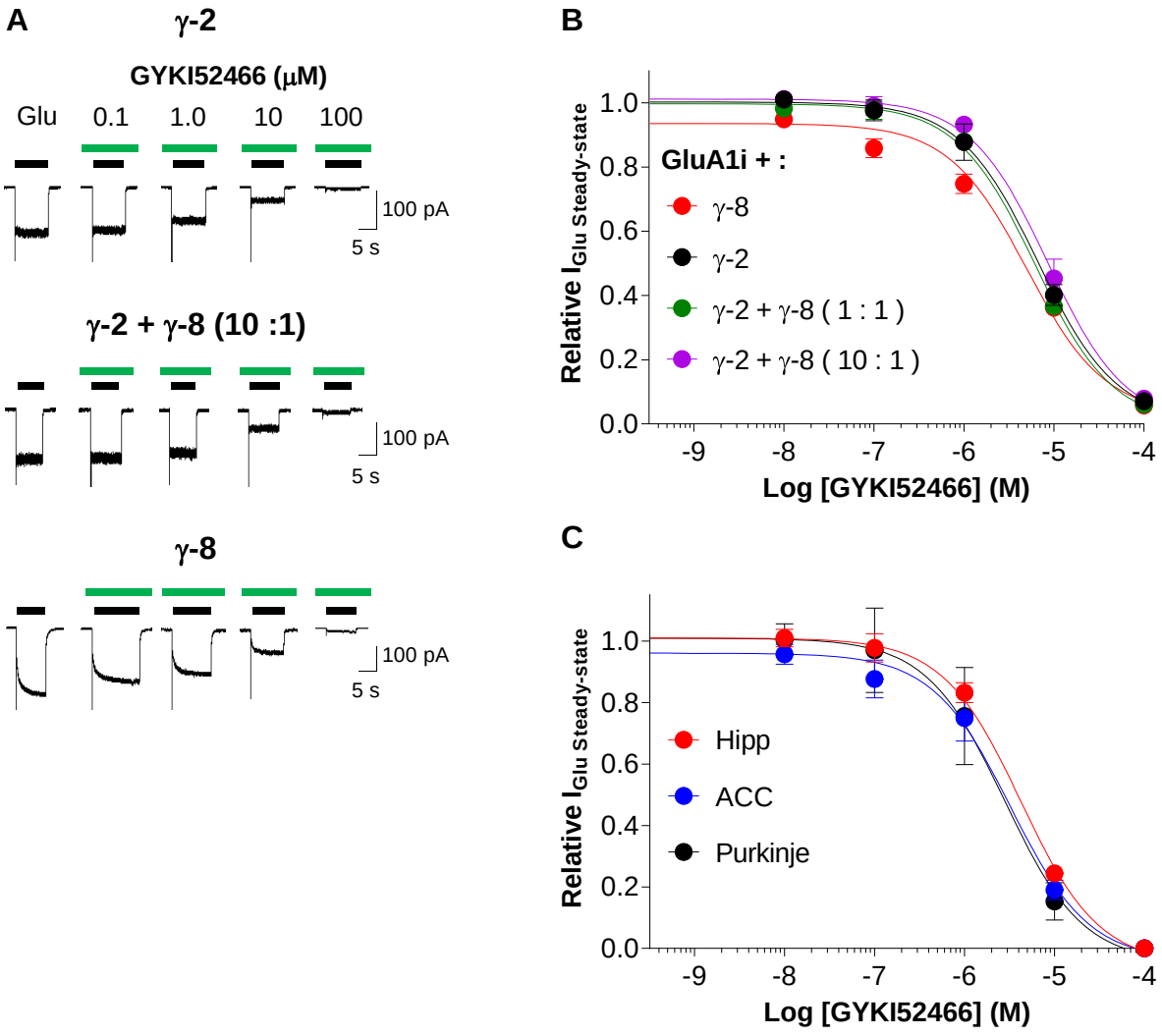

Figure 2

JPET Fast Forward. Published on March 25, 2019 as DOI: 10.1124/jpet.118.250126
This article has not been copyedited and formatted. The final version may differ from this version.

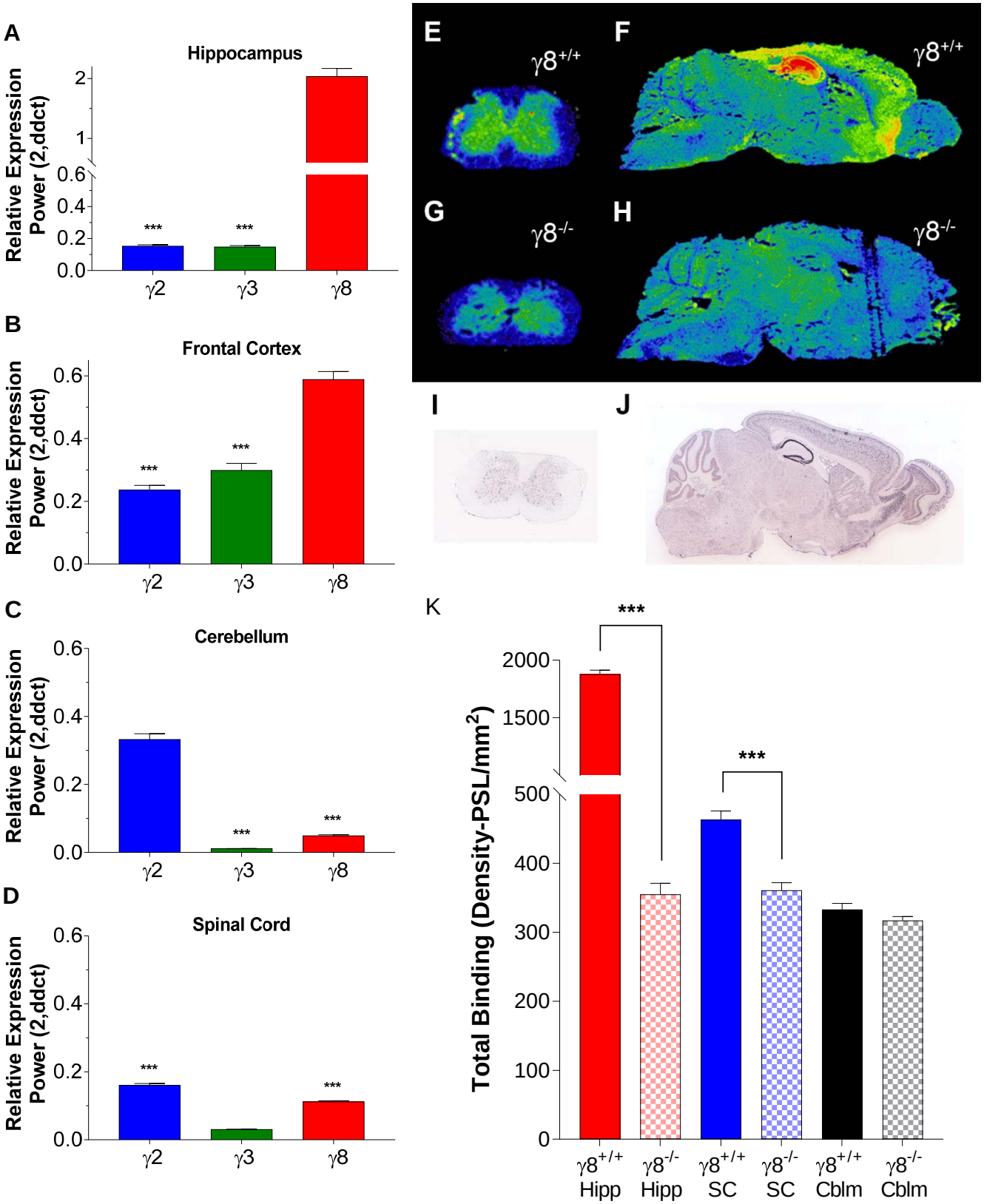

Figure 3

JPET Fast Forward. Published on March 25, 2019 as DOI: 10.1124/jpet.118.250126
This article has not been copyedited and formatted. The final version may differ from this version.

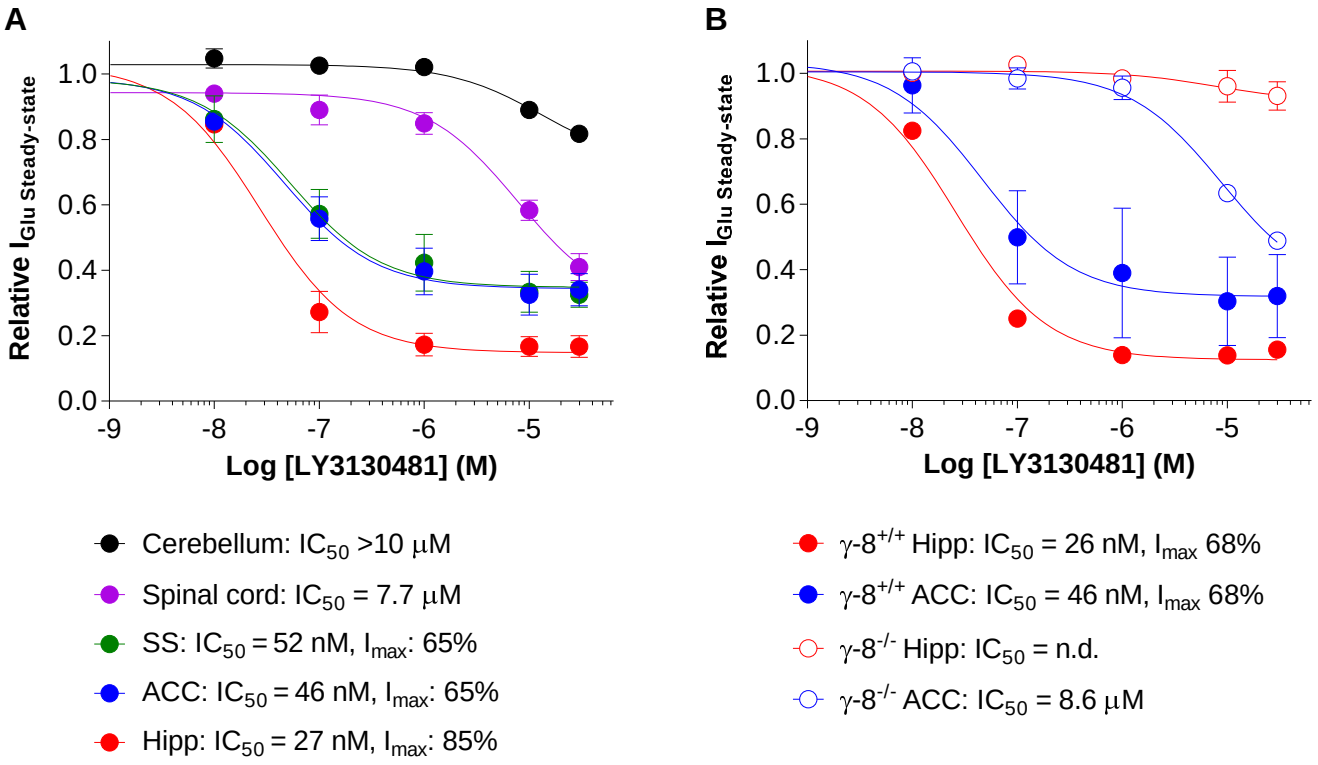

Figure 4

JPET Fast Forward. Published on March 25, 2019 as DOI: 10.1124/jpet.118.250126
This article has not been copyedited and formatted. The final version may differ from this version.

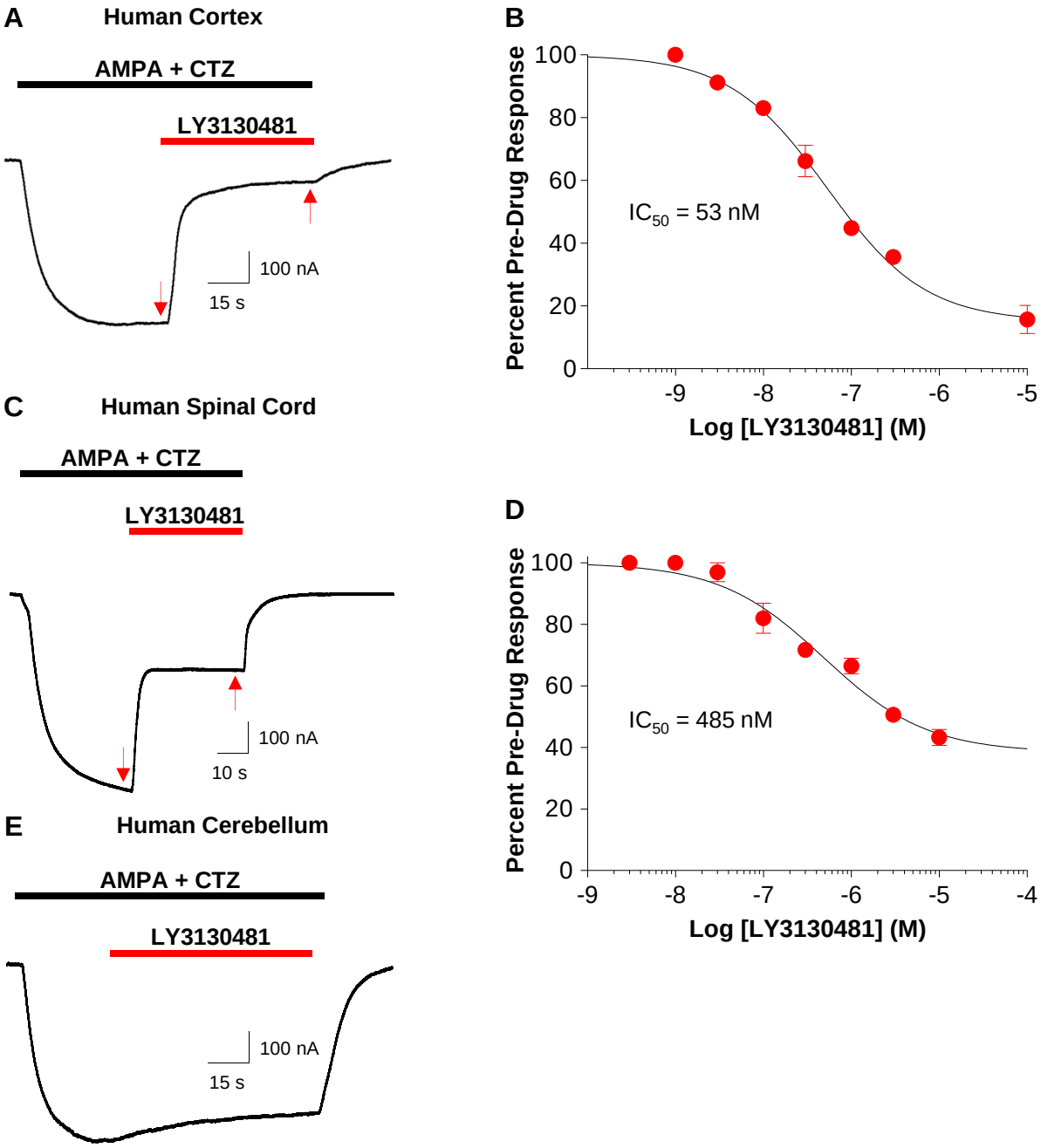

Figure 5

JPET Fast Forward. Published on March 25, 2019 as DOI: 10.1124/jpet.118.250126
This article has not been copyedited and formatted. The final version may differ from this version.

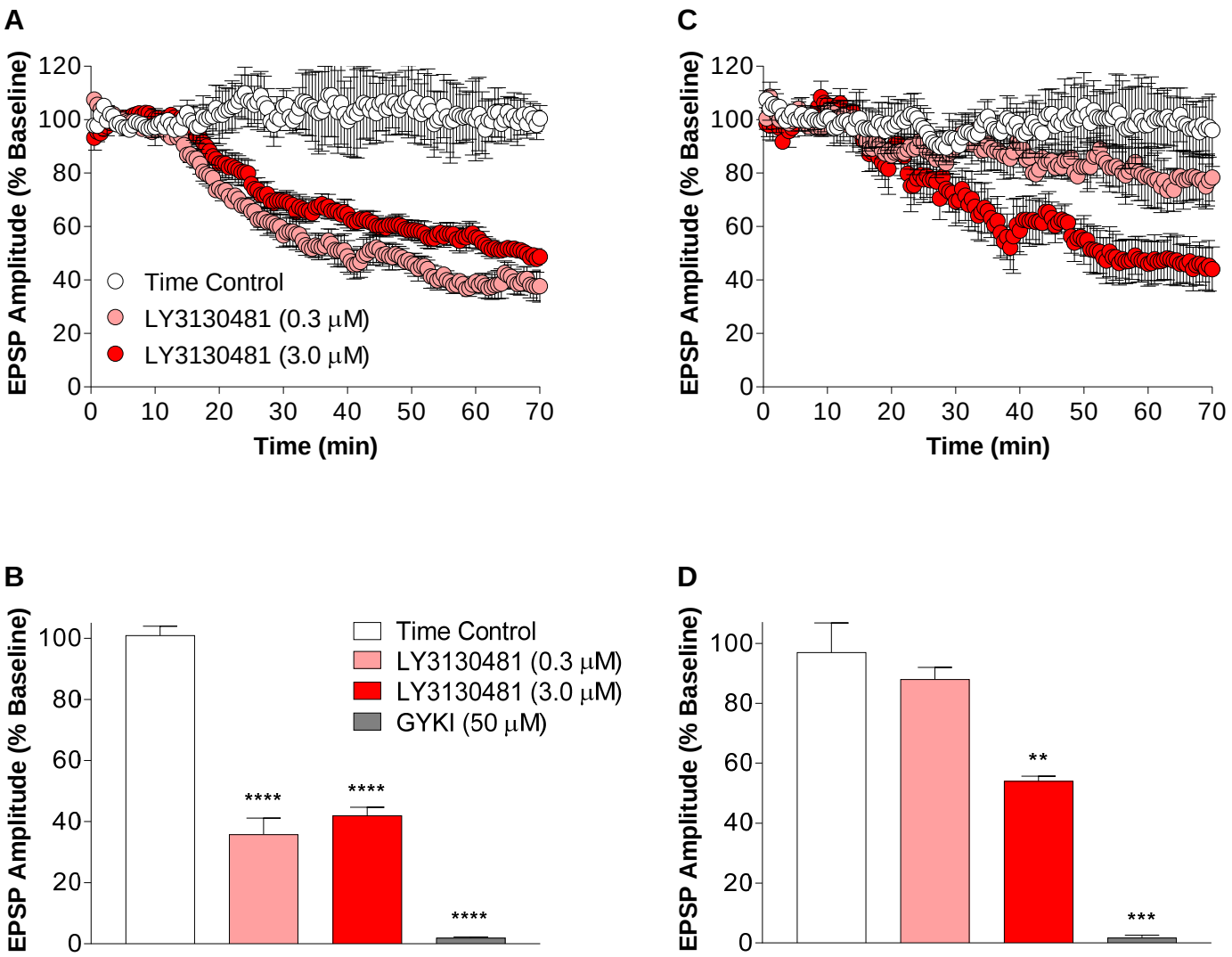

Figure 6

JPET Fast Forward. Published on March 25, 2019 as DOI: 10.1124/jpet.118.250126
This article has not been copyedited and formatted. The final version may differ from this version.

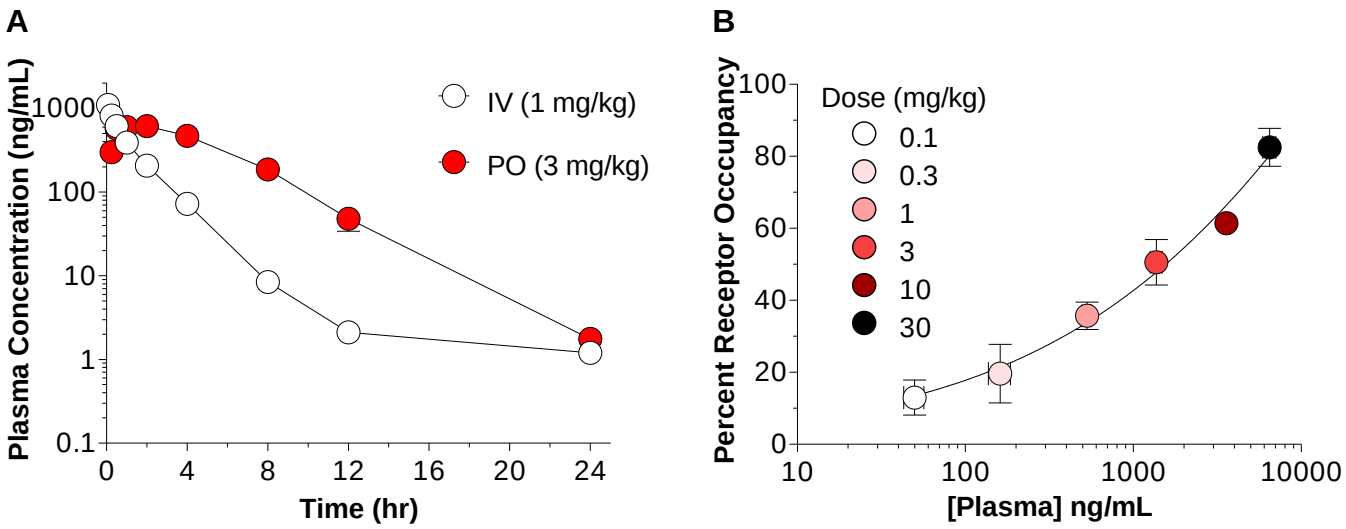

Figure 7

JPET Fast Forward. Published on March 25, 2019 as DOI: 10.1124/jpet.118.250126
This article has not been copyedited and formatted. The final version may differ from this version.

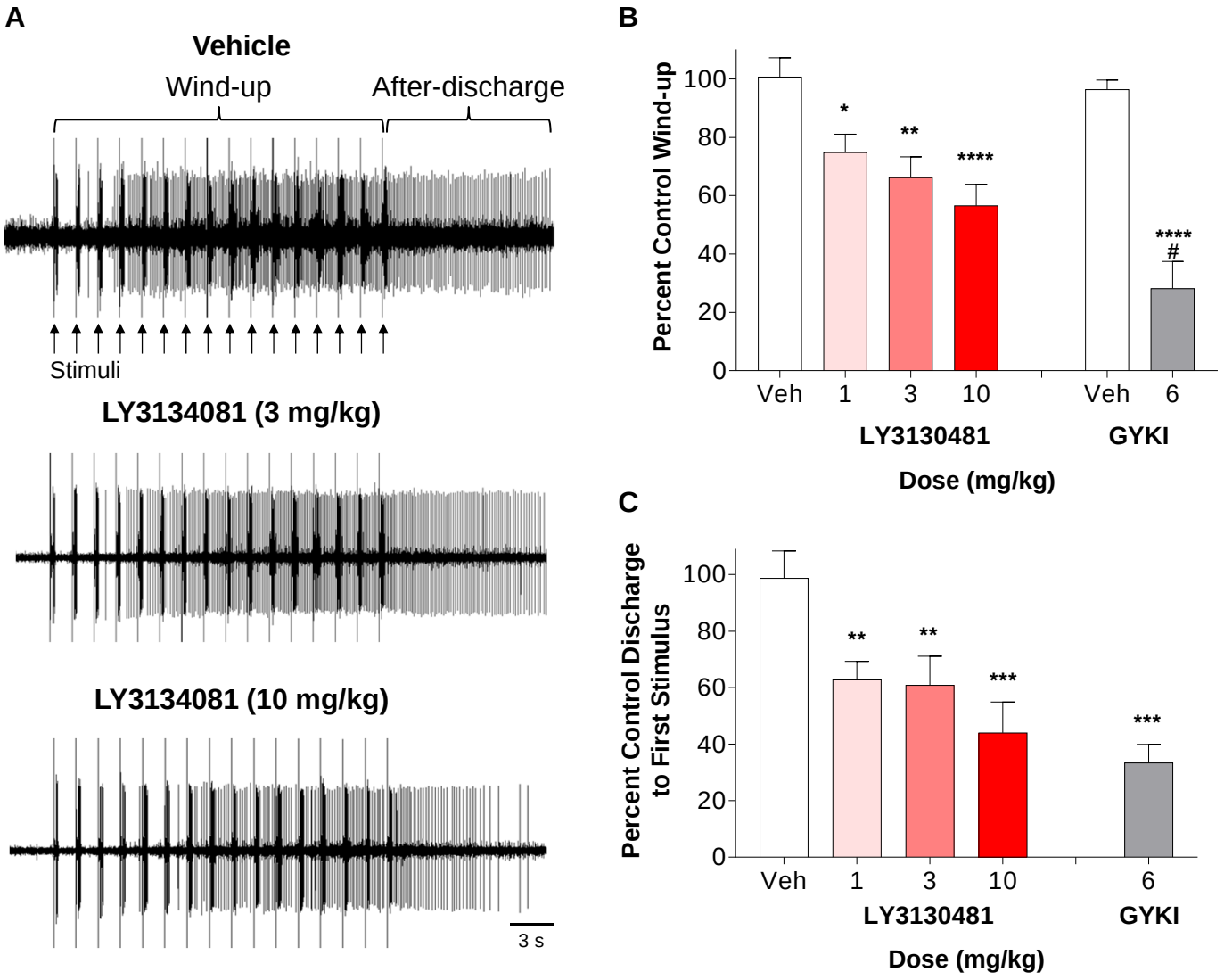

Figure 8

JPET Fast Forward. Published on March 25, 2019 as DOI: 10.1124/jpet.118.250126
This article has not been copyedited and formatted. The final version may differ from this version.

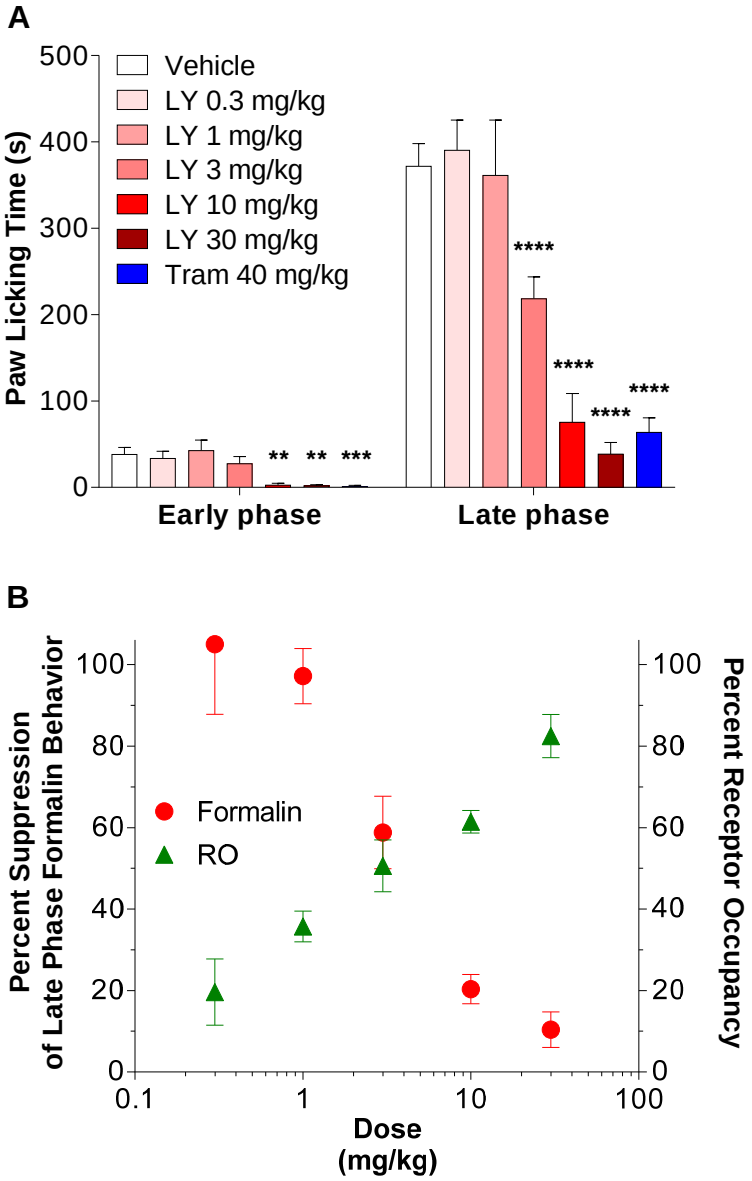

Figure 9

JPET Fast Forward. Published on March 25, 2019 as DOI: 10.1124/jpet.118.250126
This article has not been copyedited and formatted. The final version may differ from this version.

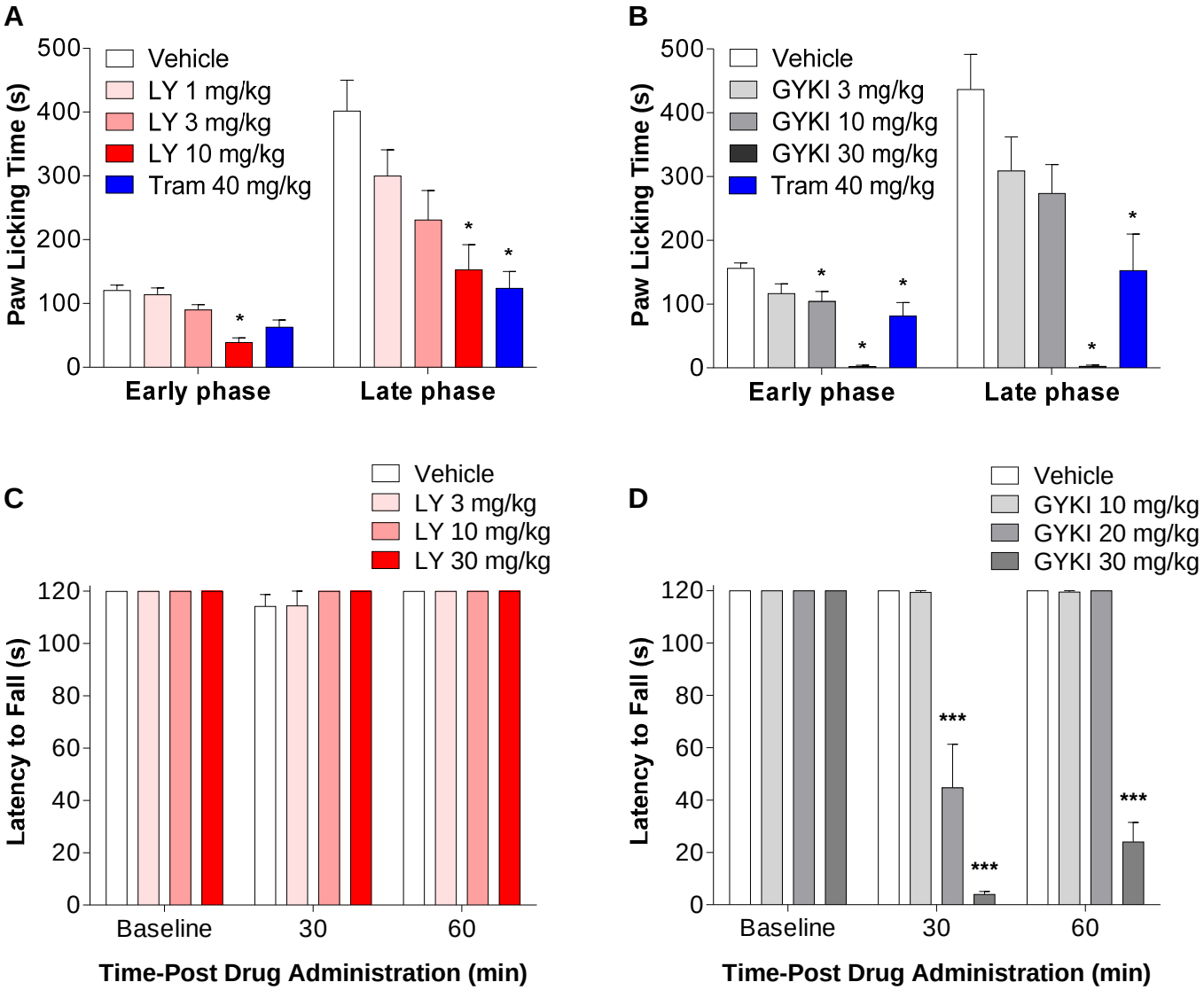

Figure 10

JPET Fast Forward. Published on March 25, 2019 as DOI: 10.1124/jpet.118.250126
This article has not been copyedited and formatted. The final version may differ from this version.

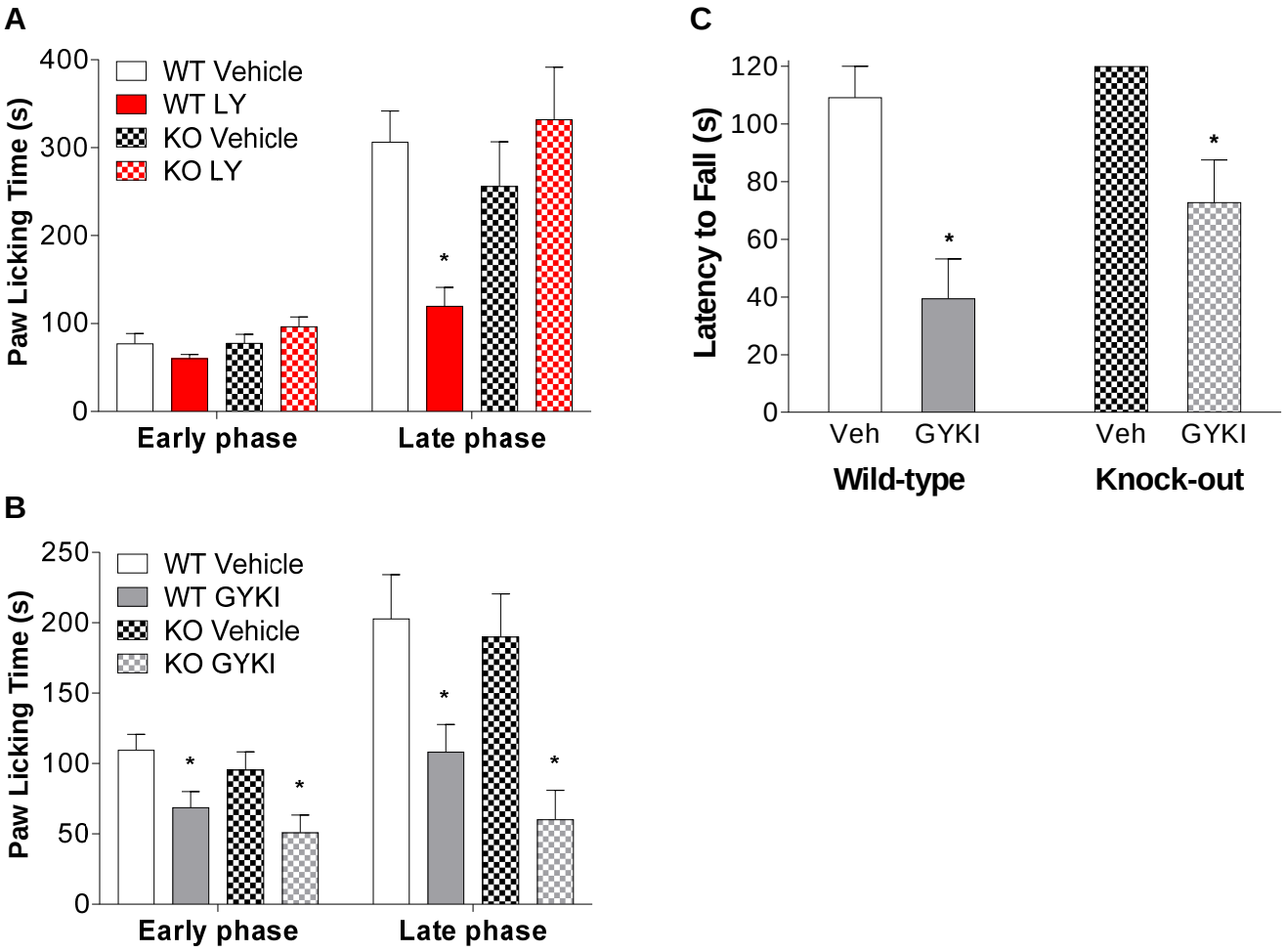

Figure 11

JPET Fast Forward. Published on March 25, 2019 as DOI: 10.1124/jpet.118.250126
This article has not been copyedited and formatted. The final version may differ from this version.

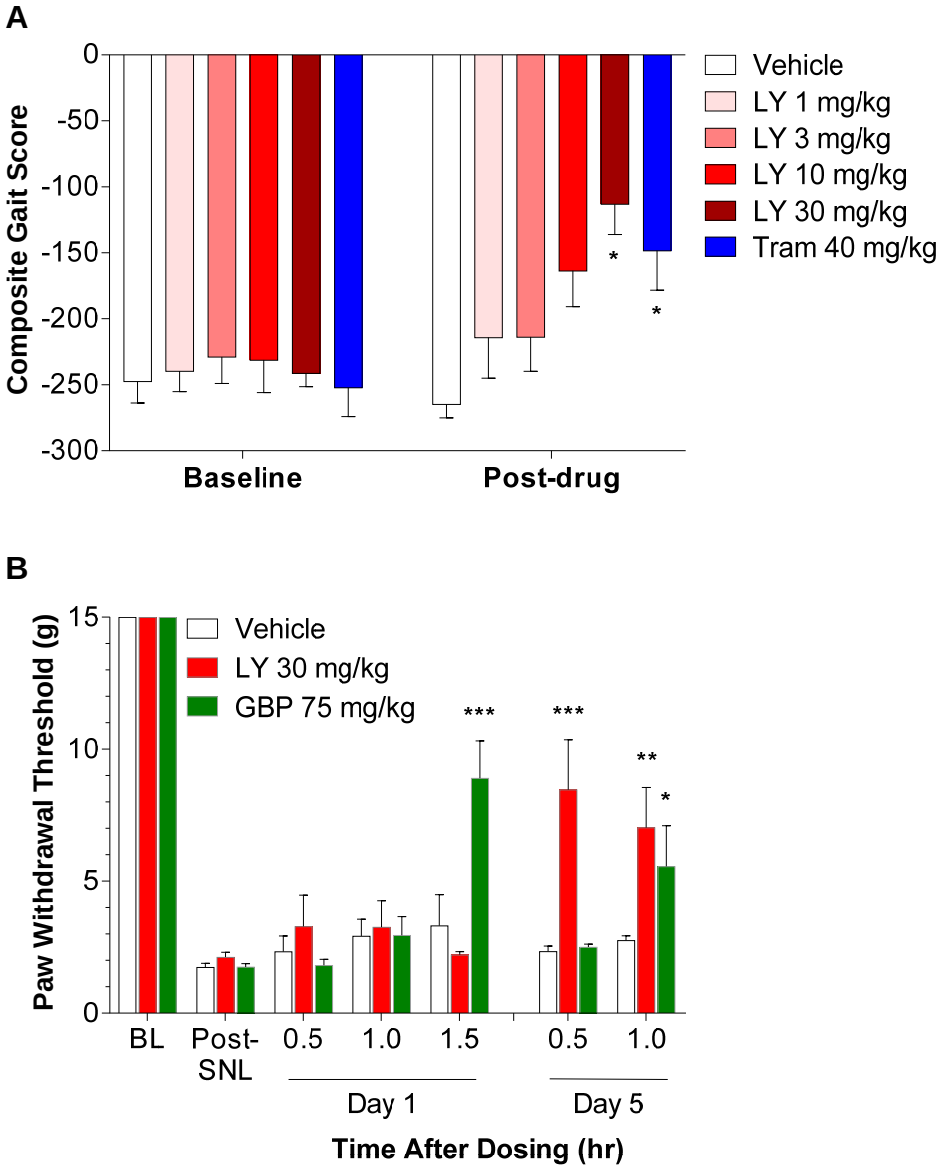

Figure 12